

Mapping benthic marine habitats featuring coralligenous bioconstructions: a new protocol approach functional to support geobiological researches research

Giuseppe Maruca^{1*}, Mara Cipriani^{1*}, Rocco Dominici¹, Gianpietro Imbrogno¹, Giovanni Vespasiano¹, Carmine Apollaro¹, Francesco Perri¹, Fabio Bruno², Antonio Lagudi², Umberto Severino², Valentina A. Bracchi³, Daniela Basso³, Emilio Cellini⁴, Fabrizio Mauri⁴, Antonietta Rosso⁵, Rossana Sanfilippo⁵, Adriano Guido¹.

¹Department of Biology, Ecology and Earth Sciences, University of Calabria, 87036, Rende, Italy;

²Department of Mechanical, Energy and Management Engineering, University of Calabria, 87036, Rende, Italy;

³Department of Earth and Environmental Sciences, University of Milano-Bicocca, 20126, Milan, Italy;

⁴Regional Agency for the Environment (ARPACAL), Regional Marine Strategy Centre (CRSM), 8890, Crotone Italy.

⁵Department of Biological, Geological and Environmental Sciences, University of Catania, 95129, Catania, Italy.

Correspondence to: Giuseppe Maruca (giuseppe.maruca@unical.it); Mara Cipriani (mara.cipriani@unical.it)

Abstract. Seabed mapping represents a very useful tool for seascape characterization and benthic habitat study, and requires advanced technologies for acquiring, processing and interpreting remote data. Particularly, acoustic instruments, such as high-resolution swath bathymetry sounder (*i.e.*, Multibeam Echosounder: MBES), allows to recognize, identify and map the extension of benthic habitats without applying invasive mechanical procedures. Bathymetry and backscatter (BS) data are crucial to perform modern habitat mapping, however they require careful end-product development and, to date, no standardized procedure exists. Although the acquisition and processing of bathymetric data follows standardized procedure (*e.g.*, Hydrographic Organization guidelines), and recent studies proposed recommendation for backscatter acquisition and processing, a broadly validated methodological approach, integrating geomorphometric analysis for benthic habitat mapping, is still lacking. In this work, a ~~protocol~~ new approach for benthic habitat mapping, with focus on coralligenous bioconstructions, was developed using the open-source software QGIS. This ~~protocol~~ methodology, tested within the Isola Capo Rizzuto Marine Protected Area (Calabria, Italy), is designed to be freely reproducible by researchers working in the field of marine ecosystem monitoring and conservation. Through the proposed mapping procedure, it is possible to: i) identify benthic habitats on selected study areas by combining bathymetry and BS data with geomorphological indices performed in QGIS; ii) quantitatively define the 2D and 3D distribution of coralligenous bioconstructions in terms of surface covered, thickness and volume. Moreover, the statistical analysis of quantitative morphometric data allowed for comparison of geometric characteristics of different coralligenous morphotypes. The obtained results, combined with improvement of minimally invasive sampling and geobiological-geochemical characterization, can contribute to the development of protocols aimed at monitoring marine bioconstructed ecosystems, many of which protected by national and international regulations due to their importance for Mediterranean biodiversity preservation, and plan actions for their protection and persistence.

1 Introduction

Bioconstructions are geobiological bodies formed in situ by growth of skeletonised organisms and represent habitats that host a great variety of benthic species. They experience a wide array of dynamic phenomena, resulting from the balance

between the action of habitat builders, dwelling organisms and bioeroders on a relatively large temporal scale over decadal to millennial timescale. Along the Mediterranean continental shelf, the most conspicuous bioconstructed habitats are represented by coralligenous build-ups (Bracchi et al., 2015, 2017, 2022; Basso et al., 2022; Cipriani et al., 2023, 2024), vermetid reefs (Picone and Chemello, 2023), sabellariid build-ups (Sanfilippo et al., 2019, 2022; Deias et al., 2023) and polychaetes–bryozoan bioconstructions (Guido et al., 2013, 2016, 2017a, b, 2019a, b, 2022), whereas cold–water corals occur in deeper settings (Rueda et al. 2019, Foglini et al., 2019). Coralligenous is known as a biocenosis complex consisting of a hard biogenic substrate primarily generated by the superimposition of calcareous red algae able to form 3D structures, supporting a high biodiversity (e.g., Ballesteros, 2006; Bracchi et al., 2022; Rosso et al., 2023; Sciuto et al., 2023; Donato et al., 2024). Although recent studies highlighted some terminological uncertainty in the definition of coralligenous habitat (e.g., Jardim et al., 2025 and references therein), within the geobiological literature the term coralligenous bioconstructions is widely and consistently adopted to indicate these biodiversity-rich, three-dimensional biogenic structures characterized by several layers of encrusting coralline algae (e.g., Ingrosso et al., 2018; Bracchi et al., 2017, 2022; Basso et al., 2022; Cipriani et al., 2023, 2024; Ferrigno et al., 2024).

Pérès and Picard (1964) and Pérès (1982) identified Coralligenous as the ecological climax stage for the Mediterranean circalittoral zone, with some bioconstructions also occurring in dim–light very shallow settings (Ballesteros, 2006; Bracchi et al., 2016; Basso et al., 2022). Coralligenous produces various morphotypes on the seafloor and plays a key role in the formation and transformation of seascape over geological time (Bracchi et al., 2017; Marchese et al., 2020). Architecture and morphology are mainly influenced by biological carbonate production, that responds to different factors, like physiography, oceanography, terrigenous supply and climate (Schlager, 1991, 1993; Betzler et al., 1997; Bracchi et al., 2017). Based upon the nature of the substrates, coralligenous morphotypes have been categorized in two main groups: i) banks, flat frameworks mainly built on horizontal substrata and, and ii) rims, structures on submarine vertical cliffs or close to the entrance of submarine caves (Pérès & Picard, 1964; Laborel, 1987; Ballesteros, 2006; Bracchi et al., 2017; Marchese et al., 2020; Gerovasileiou & Bianchi, 2021). Moreover, Bracchi et al. (2017) introduced a new classification for coralligenous morphotypes on sub–horizontal substrate using a shape geometry descriptor, in order to improve its knowledge by ensuring an objective description obtain a more objective description of these morphologies, classified in: i) tabular banks, i.e., large tabular structures with a significant lateral continuity that completely cover the seafloor, forming an extensive habitat; ii) discrete reliefs, i.e., smaller, distinct structures often arranged in clusters that do not fully cover the seafloor, leaving patches of sediment between them; and iii) hybrid banks, a category grouping morphologies intermediate between tabular banks and discrete reliefs. These structures can coalesce into a larger formation, resembling tabular banks, while still maintain individual characteristics. Hybrid banks often occur alongside other habitats, and their distribution is influenced by local sediment and hydrodynamic conditions (Bracchi et al., 2017).

Although coralligenous bioconstructions occur along almost the entire Mediterranean continental shelf, they have been mapped only in few areas and their distribution is still underestimated (De Falco et al 2010, 2022; Innangi et al 2024). In addition, as known hot spot of biodiversity, along with its low accretion rate of 0.06–0.27 mm/yr and its sensitivity to natural and anthropogenic impacts (Di Geronimo et al., 2001; Bertolino et al., 2014; Basso et al., 2022; Cipriani et al., 2023, 2024), Coralligenous is acknowledged as a priority habitat for protection under the EU Habitats Directive, is part of the Natura 2000 network (92/43/CE), and is subject to specific conservation plans within the framework of the Barcelona Convention (UNEP–MAP–RAC/SPA, 2008; UNEP–MAP–RAC/SPA, 2017). Moreover, together with other vulnerable settings (e.g., Cold–Water Corals), Coralligenous is monitored under the Marine Strategy Framework Directive (MSFD, EC, 2008; SNPA, 2024). As a result, non–destructive methods have been developed to assess the health status and ecological quality of this habitat (Bracchi et al., 2022). For all these reasons, seabed mapping can provide a

81 very useful tool for seascape characterization and mapping of Coralligenous and other vulnerable habitats (Chiocci et al.,
82 2021). In particular, acoustic instruments, such as high-resolution swath bathymetry sounder, side scan sonar and acoustic
83 profiling, enable the quick detection and identification of benthic habitats and thus mapping their extension without any
84 direct contact that might represent a threat for these vulnerable ecosystems (Bracchi et al., 2017; Chiocci et al., 2021).
85 Several studies have demonstrated that such technologies, especially when combined with backscatter (BS) data and
86 geometric descriptors, significantly enhance the study of seafloor properties and the discrimination of benthic habitats,
87 such as coral reefs, improving the understanding of their spatial distribution and ecological significance (Fonseca and
88 Mayer, 2007, Lecours et al., 2015; Brown et al., 2012; Lamarche and Lurton, 2018; Abdullah et al., 2024).
89 In this work, a semi-automated GIS-based ~~proteool~~ **approach** for benthic habitat mapping was proposed and tested in
90 shallow coastal waters, off Capo Bianco, within the Isola Capo Rizzuto Marine Protected Area (Crotone, Southern Italy).
91 The method combines high-resolution bathymetric and ~~backscatter~~ (BS) data obtained through MBES surveys and
92 geomorphological and geomorphometric indices in order to develop innovative approaches for eco-geomorphological
93 and geobiological characterisation of the seafloor. The benthic habitat mapping ~~proteool~~ here proposed has proven capable
94 not only of identifying marine bioconstructions, but also of quantitatively defining their spatial and three-dimensional
95 distribution in terms of area, volume and height relative to the substrate from which they arise. For these reasons, the
96 procedure represents a powerful tool for accurately delineate the extension of the bioconstructions and evaluate their
97 evolution over time in response to natural and/or anthropogenic changes. Furthermore, the combination of this mapping
98 ~~proteool~~ **approach** with minimally invasive sampling systems and geobiological-geochemical characterization of marine
99 bioconstructions, may represent a potent tool for monitoring these delicate habitats.

100 **2 Methodological approach**

101 High-resolution acoustic data of the study area offshore Capo Bianco were collected during several MBES surveys (Fig.
102 1) performed between February and July 2024 as part of the project “Tech4You PP2.3.1: Development of tools and
103 applications for integrated marine communities and substrates monitoring; Action 1: Development of hardware and
104 software systems for three-dimensional detection, sampling and mapping of underwater environments”, in
105 implementation to the previous bathymetric and backscatter data acquisition and elaboration of CRSM-ARPACAL.
106 The ~~proteool~~ **approach** proposed for benthic habitat mapping and defining of spatial and three-dimensional distribution
107 of coralligenous bioconstruction is briefly shown in Figure 2. In particular, mapping operations were conducted using
108 QGIS 3.34.9 “Prizren”. The most representative morphological indices, **represented by slope and seafloor roughness**,
109 were extracted from the Digital Terrain Model (DTM). Due to the large amount of data resulting from the need to obtain
110 a high-resolution mapping of benthic habitats, backscatter and bathymetry values, together with geomorphological-
111 geomorphometric indices, were imported and queried into PostgreSQL, an open-source and free relational database
112 management system (RDBMS) capable of executing queries in SQL language.

113



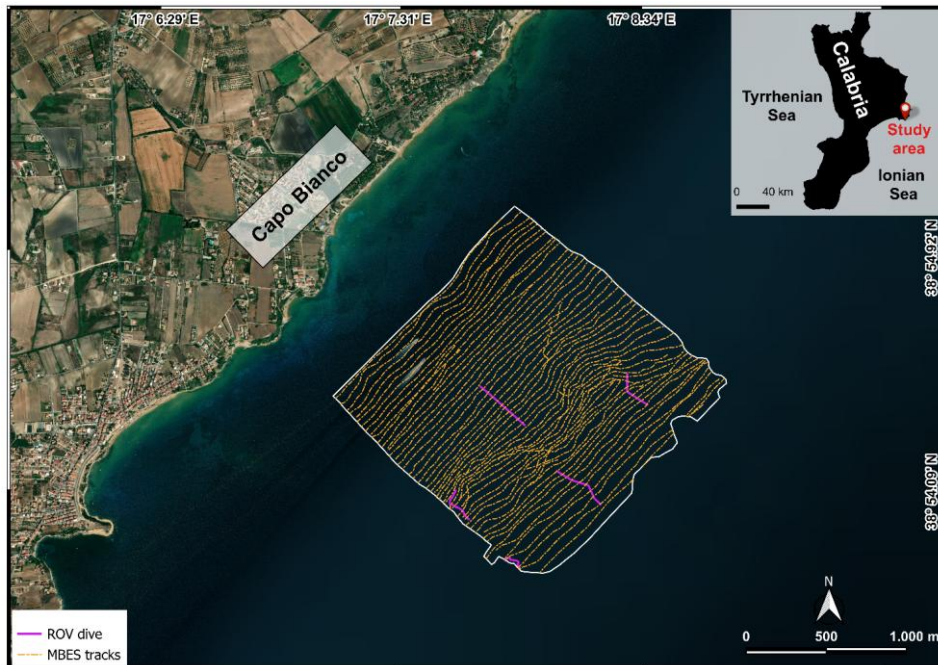


Figure 1: Study area off Capo Bianco (Calabria, Italy) and location of the MBES tracks and ROV–video transect (modified basemap from Esri World Imagery).

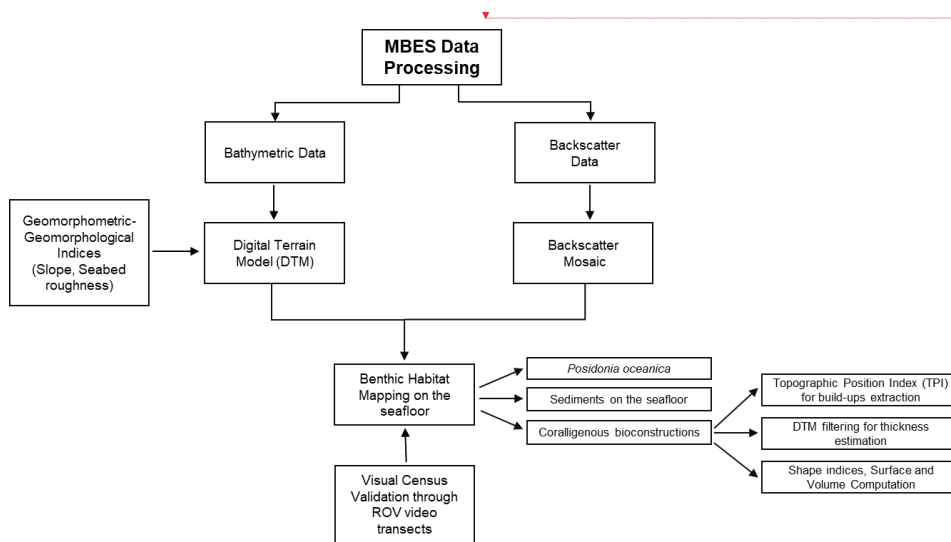
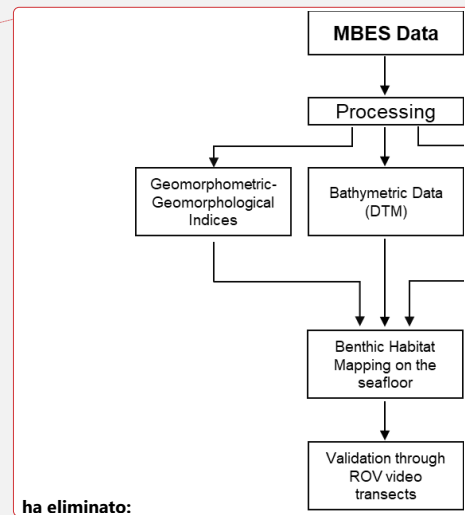


Figure 2: Conceptual model of the workflow for the development of the proposed benthic habitat mapping model approach.



ha eliminato:

123
124 Once the spatial extension and distribution of the benthic habitat have been defined by combination of bathymetric,
125 backscatter, slope and seafloor roughness data, the extraction of coralligenous build-ups was performed using the
126 Topographic Position Index (TPI), according to Marchese et al. (2020). Moreover, area, Shape Index (SI), maximum
127 diameter (Dmax) thickness and volume were calculated for each extracted polygon. Finally, the benthic habitat mapping
128 model was ground-truthed by visual analysis of ROV-video transect performed along specific paths identified in the
129 within the study area. The underwater video surveys were obtained using a VideoRay Defender equipped with a functional
130 prototype of the optical module dedicated to mapping, comprising a stereo-camera, a high-resolution camera and a
131 lightning system (Severino et al., 2023). The primary objective of this hardware is to generate high-resolution, sealed 3D
132 models through the use of a stereo-camera system. Both cameras have been meticulously calibrated to correct for optical
133 distortions, ensuring accurate and reliable data acquisition. The selected cameras were the GoPro Hero 9 Black, serving
134 as the high-resolution camera, and the Stereolabs ZED2i, serving as the stereo camera. The GoPro Hero 9 Black is a
135 small-sized action camera with a 26.3 MP CMOS sensor capable of acquiring videos at a resolution of 5120×2880 at 30
136 fps, digital stabilization, and a horizontal field of view up to 128°. The ZED2i is a stereo camera with dual 4 MP sensors
137 of 2 μm pixel size, a depth range between 0.3 m to 20 m, capable of acquiring video with a resolution of 2208×1242 at
138 15 fps, and a horizontal field of view of 110°. The stereo-camera communicates with the surface control unit by means
139 of a single-board microcomputer, a NVIDIA Jetson Nano, which supports the CUDA architecture for parallel elaboration.
140 The GoPro Hero 9 Black features Bluetooth Low Energy (BLE) and Wi-Fi communication capabilities. The acquisition
141 parameters for both cameras can be configured via the enclosure using a custom user interface accessible on the surface
142 computer.

143 2.1 Bathymetric and backscatter data

144 MBES surveys have been carried out using a pole-mounted, Norbit WBMS Basic multibeam sonar system Norbit
145 iWBMS Long Range Turnkey Multibeam Sonar System integrated with GNSS/INS (Applanix OceanMaster), operating
146 with Real Time Kinematic (RTK) corrections, ensuring high positioning accuracy during the surveys. Data were collected
147 in 46 59 tracks with a swath overlap of 20–40 % performed at an average speed of 4.5 knots. Several sound velocity
148 profiles A total of three sound velocity profiles per day were collected before starting the acquisition using a Sound
149 Velocity Profiler–Valeport miniSVP. Considering the absence of freshwater inputs and the relative stability of the water
150 column across the depth range, this was deemed sufficient to ensure reliable sound speed correction.

151 The MBES survey provided both bathymetry and BS data. The processing of MBES bathymetric data was performed
152 using QPS Qimera and included corrections for tide, heading, heave, pitch and roll. The correction of sound velocity was
153 carried out using profiles obtained with the Valeport miniSVP. Subsequently, the soundings underwent manual cleaning
154 to remove spikes. The bathymetric dataset was exported as a 32-bit raster file with a cell size of 0.05 m.

155 BS data were processed using QPS Fledermaus, and the final output was exported as an 8-bit raster file with 0.05 m cell
156 size. Backscatter data were processed using QPS Fledermaus, based on time series data and applying standard corrections
157 for sonar configuration (e.g., source level, beam pattern, receiver gain) and environmental factors (e.g., absorption, slant
158 range, footprint geometry). The processing was performed according to the general principles outlined in the Backscatter
159 Working Group guidelines (Lurton et al., 2015), which provide detailed recommendations for the acquisition, correction,
160 calibration and processing of MBES-backscatter data. The final output, exported as an 8-bit raster file with a 0.05m cell
161 size, was used to extract morphological and acoustic patterns of the seafloor.

162 2.2 Geomorphological–geomorphometric indices

163 Geomorphologic and geomorphometric indices were obtained using SAGA (System for Automated Geoscientific
164 Analysis; Conrad et al., 2015) Next Gen Provider and GDAL plugins. In particular, the slope, expressed in degrees, was
165 calculated using the dedicated function implemented in the GDAL plugin using a ratio of vertical units to horizontal of
166 1.0 and applying the Zevenbergen–Thorne formula instead of the Horn’s one. Indeed, the Zevenbergen–Thorne method
167 (1987), that considers a second–order finite difference, is more dedicated to geomorphological applications as it uses a
168 particular weighting scheme that emphasizes changes in curvature and terrain shape. Seabed roughness was assessed
169 using the Terrain Roughness Index (TRI), which provides a quantitative measure of terrain heterogeneity (Riley et al.,
170 1999). In particular, TRI values close to 0 indicate fairly regular and uniform surfaces, moderate TRI values correspond
171 to more pronounced irregularities, while high TRI values identify rugged morphologies and/or complex structures on the
172 seafloor. TRI was calculated using SAGA module “Terrain Roughness Index” with the following settings: circle as search
173 mode; a search radius of 0.5 map units (m.u.); gaussian weighting function: a value of 3.00 for the power; a bandwidth
174 of 75.00. The values of these parameters were selected through a trial-and-error method in order to best highlight the
175 heterogeneity of the seabed.

176 2.3 Topographic Position Index

177 The Topographic Position Index (TPI) was calculated at the finest possible scale (min radius: 1.00 m.u.; max radius: 5.00
178 m.u.) according to the DTM resolution and using a Power of 3.00 and a Bandwidth of 150.00. TPI is a morphometric
179 parameter based on neighbouring areas useful in DTM analysis (Wilson and Gallant, 2000). Specifically, positive TPI
180 values indicate areas that are higher than the average of their surroundings, TPI values near zero correspond to flat areas
181 or region with a constant slope, while negative TPI values represent areas lower than their surroundings. In order to
182 facilitate the extraction of coralligenous build–ups from surrounding seafloor and reduce the occurrence of artifact, a TPI
183 threshold of 0.2 was used and all the grid cells below this value were not considered as coralligenous bioconstructions.
184 TPI scale (1.00–5.00 m.u.) and value (0.2) were chosen through a trial-and-error approach in order to preserve the high
185 resolution of the extraction which is crucial for accurate volume computation.

186 2.4 DTM filtering

187 TPI parameters extracted the distribution of the coralligenous build–ups with high–resolution in terms of perimeter
188 boundary. The thickness calculation for each coralligenous build–up was developed by the creation of a “reference
189 surface” (without build–ups) using the SAGA “DTM Filter (Slope–Based)” tool implemented in QGIS 3.34.9. This tool
190 uses concept as described by Vosselman (2000) and can be used to filter a DTM, categorizing its cell into ground and
191 non–ground (object) cell. A cell is considered ground if there is no other cell within the kernel radius where the height
192 difference exceeds the allowed maximum terrain slope at the distance between the two cells. The thickness estimation of
193 each coralligenous build–up was obtained by subtracting the average depth of each polygon extracted using TPI from the
194 average depth value of the reference surface at that specific zone.

195 After estimating the height of each build–up relative to the seabed on which it developed, the Shape Index (SI–McGarigal
196 et al., 1995) was calculated using the module “Polygon Shape Indices” of SAGA in order to describe a seafloor landscape
197 characterized by distinct Coralligenous morphotypes. Finally, covered surface and volume of each polygon were
198 calculated using vector field operation implemented into QGIS.

199 3 Geological setting

200 The study area, located offshore Capo Bianco (Isola Capo Rizzuto, Calabria, Italy), belongs to the Crotone Basin (CB)
201 (Fig. 3). The CB is the widest Neogene basin of the Calabria region, in part partly exposed along the Ionian coast and in
202 part documented offshore. It represents a segment of the Ionian fore arc basin located on the internal part on the inner
203 portion of the Calabrian accretionary wedge (Cavazza et al., 1997; Bonardi et al., 2001; Minelli and Faccenna, 2010). The
204 basin infill, developed within the context of rollback subduction, was controlled by south-eastward migration of the
205 Calabrian arc and the opening of the Tyrrhenian Sea (Serravallian-Tortonian onward) (Malinverno and Ryan, 1986;
206 Faccenna et al., 2001; Milia and Torrente, 2014). The basin infill is structured into several distinct tectono-stratigraphic
207 sequences, which reflect an extensional to transtensional tectonic regime, occasionally interrupted by transpressional to
208 compressional events (Malinverno and Ryan, 1986; Faccenna et al., 2001; Reitz and Seeber, 2012; Zecchin et al., 2012;
209 Massari and Prosser, 2013; Milia and Torrente, 2014).

210 Since the mid-Pleistocene, this region experienced a significant uplift (Westaway, 1993; Westaway and Bridgland, 2007;
211 Faccenna et al., 2011; 0.70-1.25 m/ky; Zecchin et al., 2004), which, combined with glacio-eustatic sea level fluctuations,
212 led to the formation in the Crotone Peninsula of five orders of marine terraces in the Crotone Peninsula along the Ionian
213 coast of Calabria (Palmentola et al., 1990; Westaway, 1993; Westaway and Bridgland, 2007; Santoro et al., 2009;
214 Faccenna et al., 2011; Bracchi et al., 2014; Santagati et al., 2024). Zecchin et al. (2004) recognized five orders of terraces
215 in the Crotone peninsula, considering a regional uplift of 0.70-1.25 m/ky. The terraces are spread out along the southern
216 Crotone area and are unconformably transgressive on which unconformably overlie the Piacenzian-Calabrian marly clays
217 of the Cutro Formation (Zecchin et al., 2004).

218 The Cutro Terrace (1st order terrace), represents the oldest and most elevated terrace in the Crotone area, and has been
219 ascribed to MIS 7 (ca 200 kyr) (Zecchin et al., 2011). It is a mixed marine to continental terrace, consisting of the products
220 resulting from the succession of two different sedimentary cycles: i) carbonate sedimentation, transitioning into algal
221 build-ups and biocalcarene passing into shoreface and foreshore sandstones and calcarenite; ii) predominantly
222 siliciclastic sediments, comprising shoreface, fluvial channel fill, lagoon-estuarine and lacustrine deposits (Zecchin et al.,
223 2011); ascribed to MIS 7 by Zecchin et al. (2011), is a mixed marine to continental terrace, consisting of the products of
224 carbonate (algal build-ups and biocalcarene passing into shoreface and foreshore deposits) to siliciclastic (shoreface,
225 fluvial channel fill, lagoon-estuarine and lacustrine deposits) sequences (Zecchin et al., 2011).

226 The 2nd order is represented by the Campolongo-La Mazzotta terrace, ascribed to MIS 5e by Maunz and Hassler (2000).
227 These deposits are mainly composed of bioclastic and hybrid sandstones westward and by mostly siliciclastic sandstones
228 eastwards. Bioclastic deposits and local algal patch reefs, which also contain small colonial corals, are found on La
229 Mazzotta Hill (Zecchin et al., 2011). (MIS 5e), represented by the Campolongo-La Mazzotta terrace, is characterized by
230 bioclastic and siliciclastic sandstones, with local bioclastic deposits and algal patch reefs (Maunz and Hassler, 2000,
231 Zecchin et al., 2011).

232 The Le Castella-Capo Cimiti terrace (3rd order terrace), was probably associated to the MIS 5c (Maunz and Hassler, 2000;
233 Zecchin et al., 2004; Nalin et al., 2012). The upper Pleistocene cover thins down northward of Capo Cimiti, along the
234 present coastline, and is located between 10 m and 65 m of elevation due to normal fault displacement. Carbonate
235 sediments, represented primarily by algal reefs and secondarily by bioclastic to hybrid sandstones, extensively occur in
236 the eastern and central parts of the terrace. To the west, bioclastic deposits of lower to upper shoreface environments
237 dominate (Zecchin et al., 2004; Nalin et al., 2012); probably associated to the MIS 5c (Maunz and Hassler, 2000), shows
238 extensive algal reefs and shoreface deposits, with elevations variation due to normal fault displacement (Zecchin et al.,
239 2004; Nalin et al., 2012).

240 The Capo Colonna marine terrace (4th order terrace), consists of a planar surface gently inclined eastward, with a
 241 sedimentary cover quite continuously exposed along the northern coast of the promontory and covered, in its proximal
 242 segment, by a wedge of colluvium tapering eastward (Bracchi et al., 2014). The terrace deposits correlate either with MIS
 243 5.3 (ca 100 ka; Palmentola et al., 1990; Zecchin et al., 2004, 2009), or MIS 5.1 (ca 80 ka; Gliozzi 1987; Belluomini et al.,
 244 1988; Nalin et al., 2006; Nalin & Massari, 2009). correlated to MIS 5.3 (Palmentola et al., 1990; Zecchin et al., 2004,
 245 2009), or MIS 5.1 (ca 80 ka; Gliozzi 1987; Belluomini et al., 1988; Nalin et al., 2006; Nalin & Massari, 2009), consists
 246 of a planar surface with a sedimentary cover overlaid by a wedge of colluvium tapering (Bracchi et al., 2014).
 247 The Le Castella marine terrace (5th order terrace) is the youngest. Its deposits, exceptionally well exposed along present-
 248 day coastline, form an unconformity bounded, transgressive-regressive cycle, similar to those observed in other terraces
 249 of the Crotone area (Nalin et al., 2007; Nalin & Massari, 2009; Zecchin et al., 2010; Bracchi et al., 2014; Bracchi et al.,
 250 2016). Zecchin et al. (2004, 2010) identified two different facies for coralline algal build-ups and associated bioclastic
 251 deposits in the lower portion of the cycle. The age of the Le Castella marine terrace deposits remains debated: indeed,
 252 these deposits have been correlated with MIS 5.3 (Gliozzi, 1987), MIS 5.1 (Palmentola et al., 1990) and MIS 3 (Zecchin
 253 et al., 2004; Mauz & Hassler, 2000; Santagati et al., 2024). records an unconformity-bounded transgressive-regressive
 254 cycle (Nalin et al., 2007; Nalin & Massari, 2009; Zecchin et al., 2010; Bracchi et al., 2014; Bracchi et al., 2016), with two
 255 different facies for coralline algal build-ups and associated bioclastic deposits in the lower portion (Zecchin et al., 2004,
 256 2011). The age of these deposits remains debated, as they have been correlated with MIS 5.3 (Gliozzi, 1987), MIS 5.1
 257 (Palmentola et al., 1990) and MIS 3 (Zecchin et al., 2004; Mauz & Hassler, 2000; Santagati et al., 2024).
 258 The marine terraces exposed in emerged portion near the study area demonstrated extensive carbonate production due to
 259 the development of algal bioconstruction throughout the Late Pleistocene. This production also appears to currently affect
 260 the seafloor. However, although the onshore portion of the CB has been well studied, its offshore extension is still less
 261 known (Pepe et al., 2010). Nevertheless, data from the MaGIC Project related to Sheet 39 “Crotone” covered a vast area
 262 extending from the Neto Submarine Canyon to the Capo Rizzuto Swell. In this section, the continental shelf reaches up
 263 to 7 km wide, with the shelf break located at depths of 80–120 m. The slope encompasses the southern portion of the Neto
 264 Canyon headwall and the Esaro Canyon along with its tributaries. The average continental slope gradient is less than 5°
 265 and is characterised by an undulating morphology including the Luna and the Capo Rizzuto Swell. The southern section
 266 of the sheet covers the offshore extension of the Crotone forearc basin (Chiocci et al., 2021). This work aims to enhance
 267 the understanding of the Crotone Basin offshore features, with focus on underwater bioconstructed habitats.
 268

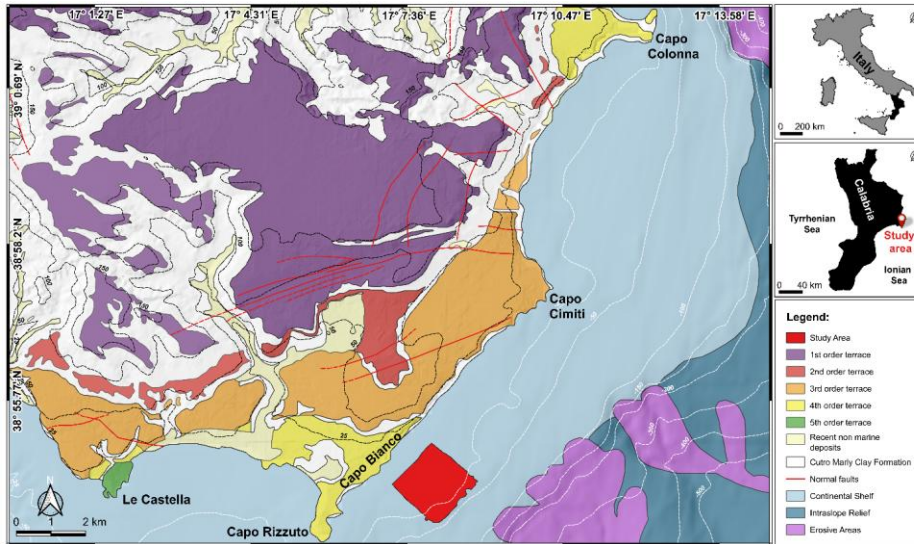


Figure 3: Conflated geological map of the Crotona peninsula, with the indication of the five order terraces (modified from Bracchi et al., 2014), and physiographic domains identified offshore the area in the frame of the MaGIC Project (modified from Chiozzi et al., 2021).

4 Results

4.1 Morphological and morpho-acoustic characteristics of the seafloor

The comparison between bathymetric (Fig. 4A) and backscatter (Fig. 4B) data with those related to slope (Fig. 4C) and seafloor roughness (Fig. 4D) allowed for the definition of the morphological and morpho-acoustic characteristics of the study area off Capo Bianco (Calabria, Italy) and the identification of the benthic habitats. In particular, bathymetric data revealed a seafloor with depths ranging from -7.3 m to -49.5 m (Fig. 4A). The transition towards the deeper areas is not gradual but shows an evident break in slope (starting from about -15m depth), especially in the central zone of the study area. The shallower portion is characterized by widespread irregularities, while the deeper areas appear generally more regular, with less pronounced variations. Slope analysis (Fig. 4C) reveals maximum values (up to about 80°) along the break in slope, highlighting a steep and well-defined margin. The surrounding areas show lower slopes, with scattered peaks associated with seafloor irregularities. The Terrain Ruggedness Index showed: i) a higher roughness along the break in slope (where the highest TRI values were recorded) and in its immediate vicinity; ii) the presence of scattered roughness associated with irregularities on the seafloor (Fig. 4D).

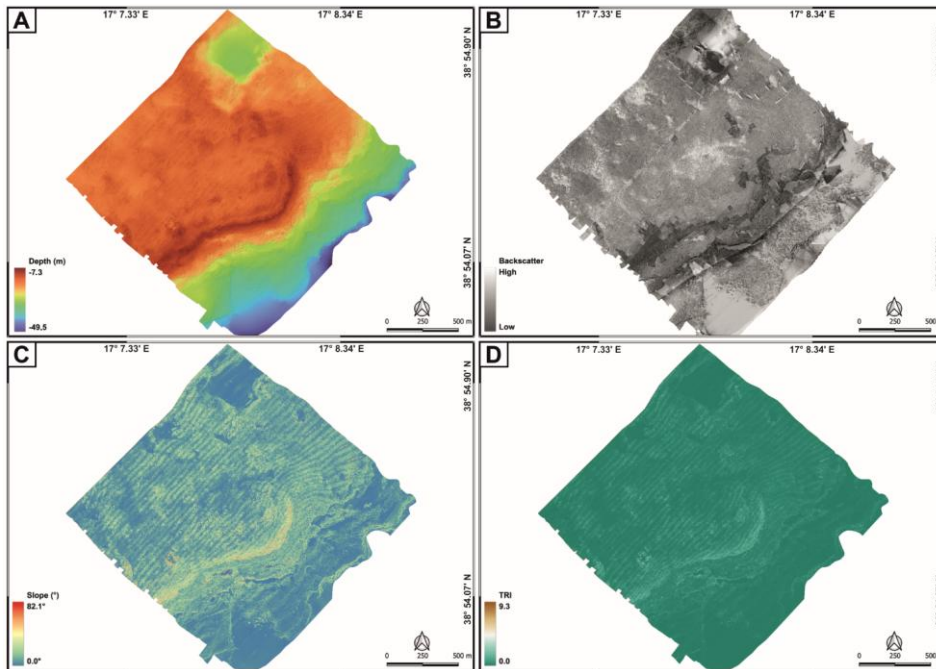


Figure 4: Geomorphological characters of the study area expressed through processed bathymetric (A), backscatter (B) data and geomorphometric indices, like slope (C) and Terrain Roughness Index (D).

Combining bathymetric and backscatter (Fig. 4B) data with slope and seafloor roughness values, different morpho-acoustic features were identified (Fig. 5):

- *Posidonia oceanica* meadows, characterized by an intermittent speckled fabric of moderate backscatter. *Posidonia* covers seabed areas characterized by low slopes and slight roughness, spanning a depth range from about -6 m to -25 m. In the depth range from -15 m to -25 m, analysis of ROV-video transects showed that *Posidonia* meadow forms a mosaic with the coralligenous habitat;
- banks of Coralligenous, characterized by a complex fabric of moderate to low backscatter. They covered areas characterized by moderate to high slopes and medium to high roughness, spanning a depth range from about -15 m to -25 m;
- discrete coralligenous build-ups surrounded by medium to coarse sediment and maerl are characterized by a dotted pattern of moderate backscatter. They covered areas characterized by low slopes and medium roughness and occupy the area between the end of the banks and the final depth of the MBES survey, at approximately -40 m depth;
- fine to medium sediment, characterized by homogeneous pattern of medium to high backscatter. It covers scattered portions throughout the study area at various depths and is characterized by very low TRI values.

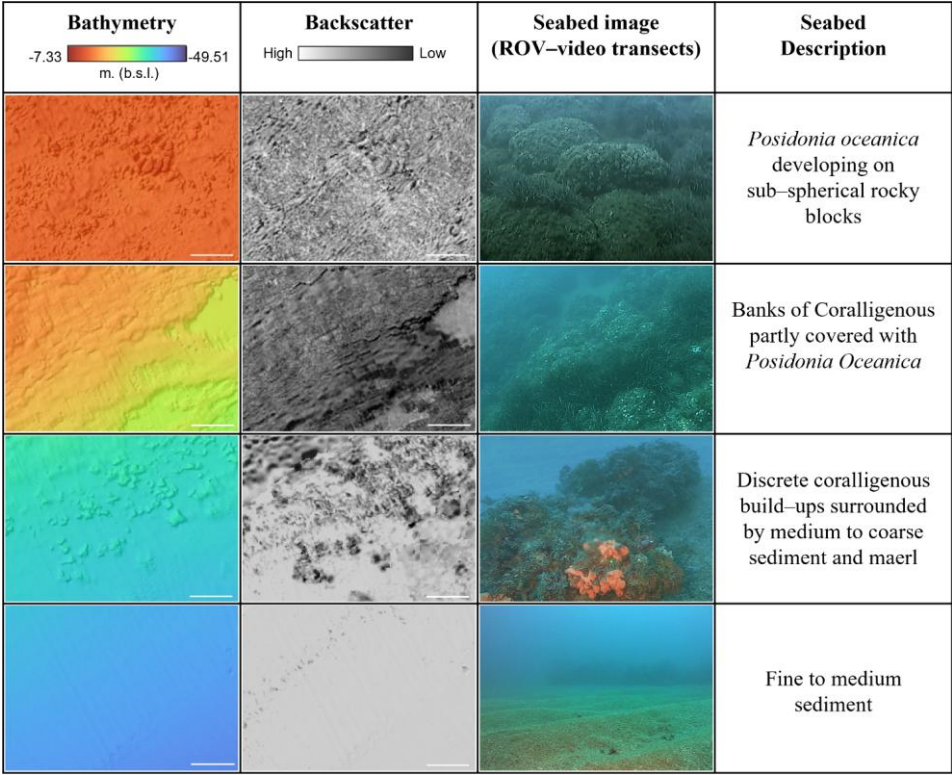


Figure 5: Morpho–acoustic features identified by bathymetric and BS data, together with ROV videos interpretation. White scale bar is 20 m.

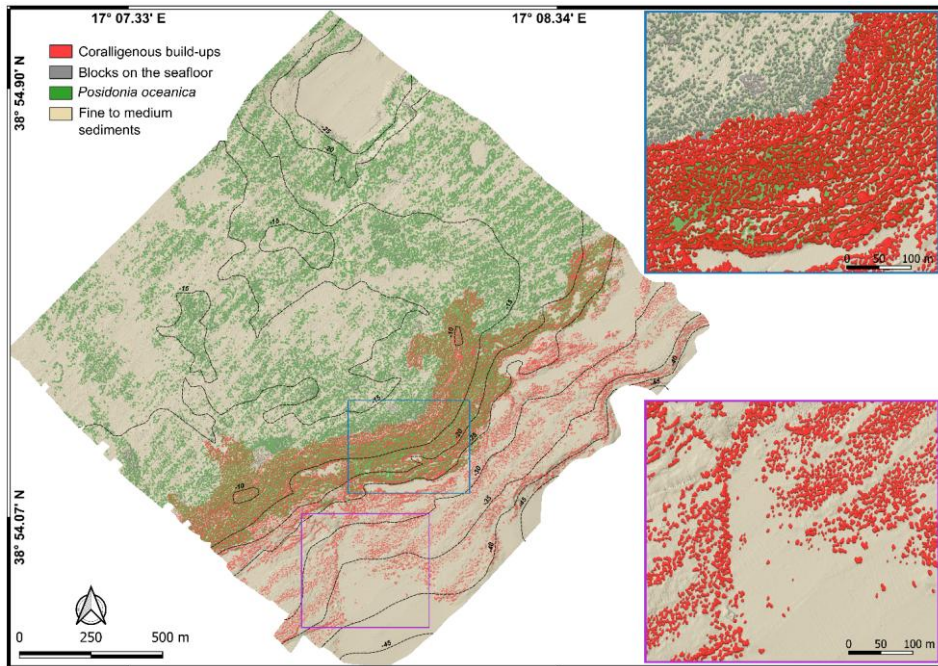
The combination of the various morpho–acoustic features enabled the identification of four main benthic habitats (Fig. 6): i) *Posidonia oceanica* meadows; ii) mosaic of coralligenous and *Posidonia*; iii) Coralligenous *sensu stricto* (*i.e.*, bioconstructions that are not spatially intermixed with *Posidonia oceanica*); iv) fine to medium sediment.

The *Posidonia* habitat, testified by its typical BS signal (intermittent speckled fabric of moderate backscatter), dominate in shallow areas (down to about -15 m depth), where it primarily colonizes rocky substrate. In this area, ROV imagery and bathymetric data also highlight the occurrence of sub-spherical rocky blocks on the seabed, often surrounded by *Posidonia oceanica* (Fig. 5).

Between -15 m and -25 m, the *Posidonia* backscatter signal gradually attenuates and coralligenous bioconstructions start to be discernible. This transitional belt, that occupies about 0.37 km², was classified as a mosaic of Coralligenous and *Posidonia oceanica*. Visual analysis of ROV-video transects, used as ground-truth, indicates that in this zone bioconstructions, mainly belonging to the banks morphotype, develop on a hard substrate that marks the widespread break in slope throughout the study area.

Below -25 m, *Posidonia* is no longer detected and the predominant benthic habitat is represented by Coralligenous *sensu stricto*. These bioconstructions, often associated with fine to medium sediment and maerl, predominantly belong to the discrete reliefs morphotype and tend to align sub-parallel to the shoreline.

325
326



327

328

329

330

331

332

333

334

335

336

337

338

339

340

341

342

343

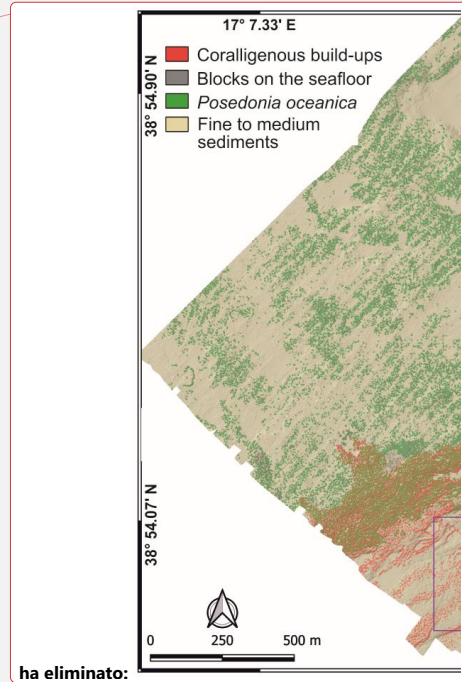
344

Figure 6: Mapping model of the underwater benthic habitats in the study area off Capo Bianco (Calabria, Italy). Note, in the blue and purple boxes, two magnifications of representative areas of the model where coralligenous bioconstructions and rocky blocks on the seabed are depicted in 2.5D.

4.2 Extraction of coralligenous build-ups

The model extracted 12384 polygons, but only 9211 positive morphologies were finally related to coralligenous build-ups considering the hillshade values and validation from ROV-video transects collected within the study area (Fig. 7A). This means that about 25 % of the polygons extracted using the TPI were found to be artifacts and manually deleted after the re-classification and the polygonization of resulting raster. According to Marchese et al. (2020), the artifacts may be due to: i) occurrence of *Posidonia oceanica* (Innangi et al., 2015) (Fig. 8A); ii) bad roll correction (Fig. 8C), creating false elongated structures; iii) artifacts concentration on DTM boundaries (Fig.8E). While artifacts of types ii) and iii) can be reduced by performing more accurate MBES surveys (i.e., larger coverage, greater overlapping, and narrower swath width), those related to *Posidonia oceanica* represent real morphological features that cannot be removed by improving survey quality.

The identification of artifacts was based on specific pattern inconsistent with expected Coralligenous morphologies, and their removal was carried out manually as part of the data cleaning process (Fig. 8B, D, F). The time required for the cleaning phase strongly depends on the quality of the survey execution, the geomorphological and ecological complexity



of the study area and the experience of the operator performing the cleaning. These factors can significantly influence the extent and efficiency of manual artifact removal.

Regarding the distinction between coralligenous bioconstructions and *Posidonia oceanica* in the mosaic area, the separation was primarily based on the characteristics of the backscatter signal. Specifically, as discussed previously, *Posidonia* is associated with a moderate, speckled acoustic texture, while coralligenous bioconstructions exhibit a more complex and spatially structured acoustic signature. These interpretations were supported by ROV video transects, which help to validate the differentiation.

~~Naturally, the time-consuming operation of filtering and manually detecting erroneous polygons could be avoided performing more accurate MBES surveys (i.e., larger coverage, greater overlapping and narrower swath width) free of artifacts.~~

4.3 Shape index, thickness, surface and volume of coralligenous build-ups

Shape Index (SI) values allowed to distinguish between banks (tabular bank *sensu* Bracchi et al., 2016; $SI \leq 2$) and discrete reliefs (discrete reliefs and hybrid banks *sensu* Bracchi et al., 2016; $SI > 2$) (Fig. 7B). Following this approach, it was possible to identify 7001 polygons belonging to the morphotype of the banks and 2210 classified as discrete reliefs. As shown in Table 1, banks have a greater average thickness (Fig. 7C) compared to discrete reliefs (0.65 m vs 0.49 m, respectively) and cover an area of 155677 m², which represents about 5.2 % of the seabed in the study area. In contrast, discrete reliefs cover only 2.6 % of the seafloor, with a surface area of 69830 m². The volume (Fig. 7D) occupied by discrete reliefs (40806 m³) is also significantly lower than that of the banks (116094 m³). This data is consistent with the fact that discrete reliefs are characterized by smaller extent and thickness compared to the banks.

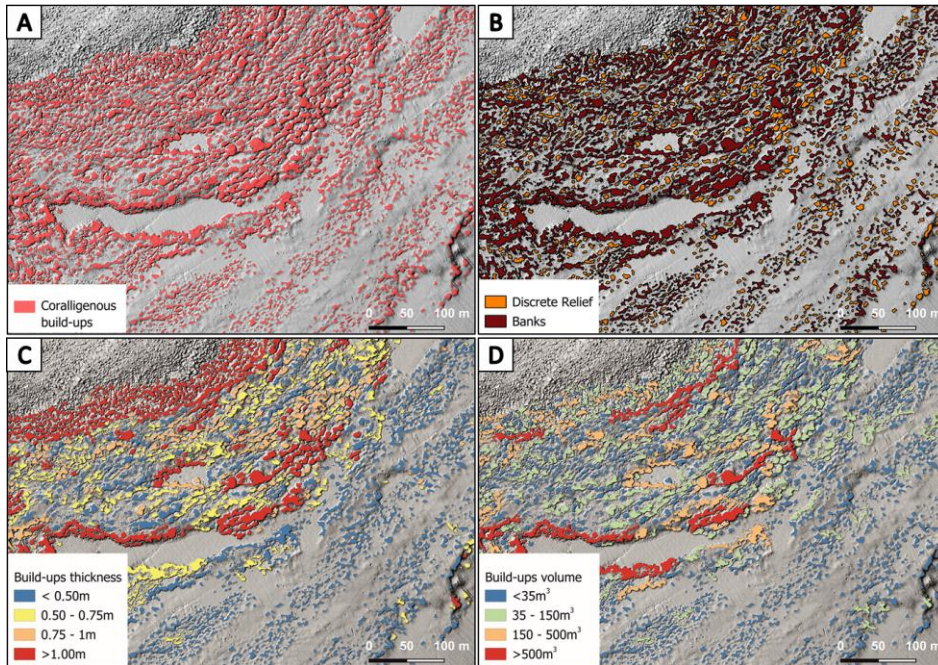


Figure 7: (A) Result of build-ups extraction using TPI. (B) Differentiation of coralligenous build-ups into discrete relief and banks based on the SI value. (C) Estimation of build-ups thickness. (D) Calculation of the volume for each coralligenous polygon.

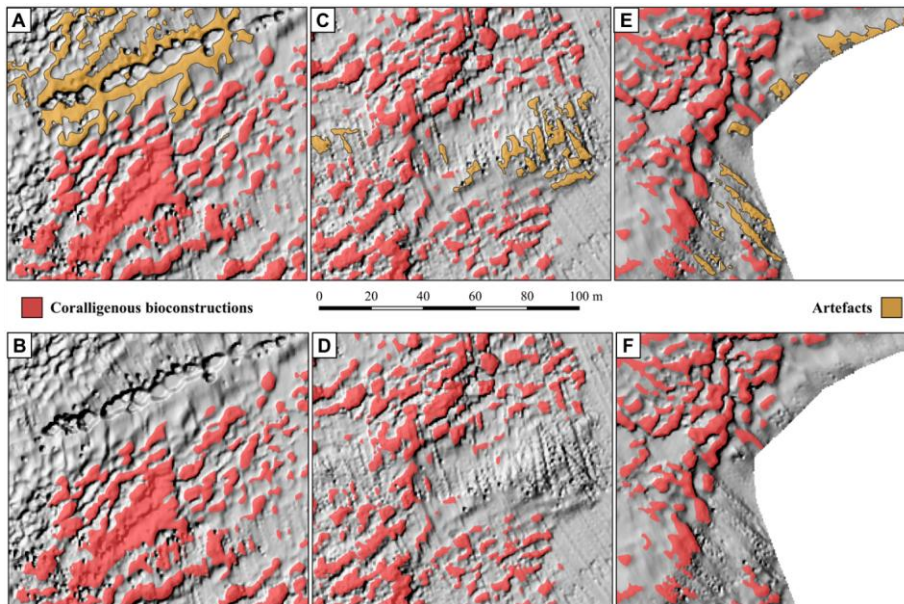


Figure 8: Examples of artifacts identified during polygon extraction and their manual removal. (A) False positive caused by the presence of *Posidonia oceanica* and (B) the same area after removal; (C) artifact due to bad roll correction and (D) corrected version; (E) artifacts at the boundary of the DTM and (F) cleaned result.

Table 1: Classification of coralligenous polygons, based on SI values, and results in terms of area and volume.

Morphotype	Shape Index Values	Average Thickness (m)	Area (m ²)	Volume (m ³)
Banks	≤ 2	0.65	155677	116094
Discrete Reliefs	> 2	0.49	69830	40806

5 DISCUSSION

Acoustic techniques, such as high-resolution swath bathymetry sounder (including backscatter), side scan sonar and acoustic profiling are optimal tools for quickly recognize and identify the extension of benthic habitats on the seabed and map their distribution without mechanical collection of samples, which would damage this delicate ecosystem (Bracchi et al., 2017).

Conventionally, the segmentation of MBES data sets is carried out manually, despite the process might be inaccurate and subjective (Cutter et al., 2003; Bishop et al., 2012). Only few studies have successfully developed object-oriented methods that use object-based image analysis (OBIA) or consider a comprehensive set of remote data to accurately characterize seabed landforms to document the extension of benthic habitat (Lucieer and Lamarche, 2011; Ismail et al., 2015; Janowski et al., 2018; Fakiris et al., 2019). However, geomorphometric techniques can objectively characterize submarine habitat and features from the shallow to deep environments (Lecours et al., 2016; Janowski et al., 2018), but a standardized technique for seafloor classification has never been developed (Micalef et al., 2012). Recently, Marchese et al. (2020) proposed a protocol that combines acoustic datasets and geomorphometric analysis, performed using ArcGIS™, in order to define the 2D and 3D complexity of coralligenous build-ups on a sector of the Apulian continental shelf and to quantify how much carbonate is deposited.

Traditionally, the segmentation of MBES data sets have been performed manually, despite the process might be inaccurate and subjective (Cutter et al., 2003; Bishop et al., 2012). Initial attempts at automation employed object-oriented methods using object-based image analysis (OBIA) or considered a comprehensive set of remote data to accurately characterize seabed landforms for documenting the extension of benthic habitat (e.g., Lucieer and Lamarche, 2011; Ismail et al., 2015; Janowski et al., 2018; Fakiris et al., 2019). More recently, the growing availability of high-resolution MBES data has encouraged the application of deep learning approaches, particularly Convolutional Neural Networks (CNNs) and Fully Convolutional Neural Networks (FCNNs), which produce pixel-wise classifications in order to create semantically segmented maps. These methods have proven effective in identifying geomorphological features such as bedrock outcrops, pockmarks, submarine dune and ridges, offering high accuracy and repeatability (Arosio et al., 2023; Garone et al., 2023). Additionally, 3D CNNs have been applied to automated denoising of MBES data, enhancing the efficiency of bathymetric data workflow (e.g., Stephens et al., 2020).

Nonetheless, a universally accepted and standardized methodology for geomorphological classification of the seafloor is still lacking. Indeed, existing approaches remain highly case-specific, depending on the study area, data quality, and research objective. Moreover, relatively limited attention has been devoted to the morphological characterization of Coralligenous bioconstructions, despite their ecological relevance. Indeed, only a few studies have attempt to map these complex biogenic structures in detail. Bracchi et al. (2017) proposed a categorization of coralligenous morphotypes on sub-horizontal substrate based on integrated acoustic data and ground-truthing, defining new morphological classes such

as tabular banks, hybrid banks and discrete reliefs across the Apulian shelf. Subsequently, Marchese et al. (2020) proposed a protocol that combines acoustic datasets and geomorphometric analysis, performed using ArcGIS™, in order to define the 2D and 3D complexity of coralligenous build-ups and to quantify how much carbonate is deposited. More recently, Varzi et al. (2022) produced a morpho-bathymetric map for the continental shelf offshore Marzamemi (Sicily, Italy) that contained quantitative description for the distribution and extent of coralligenous reefs.

The mapping protocol approach proposed in this work, based on the workflow shown in Figure 2 3, represents the first attempt to define the benthic habitat in the Isola Capo Rizzuto Marine Protected Area and to quantify the extent and morphometric characteristics of coralligenous bioconstructions present therein using exclusively open-source software during post-processing phases.

5.1 Detected habitats Spatial distribution of benthic habitats and seafloor morphology

The comparison between the bathymetric and backscatter data with the indices derived in QGIS and the model validation through ROV-video transects allowed to identify several habitats: *Posidonia oceanica* meadows, mosaic of coralligenous and *Posidonia*, Coralligenous sensu stricto, and fine to medium sediment.

The *Posidonia* habitat, testified by its typical BS signal (intermittent speckled fabric of moderate backscatter), was recognised down to 25 m water depth. *Posidonia oceanica* habitat dominates in shallow areas, down to about 15 m depth, developing primarily on rocky substrate. The seafloor is characterized by the presence of sub-spherical rocky blocks (Fig. 6), which possibly result from gravitational processes affecting the 4th order terrace emerging landwards, and pockets of fine to medium sediments.

From 15 m to 25 m, *Posidonia* BS signal gradually attenuates and Coralligenous bioconstructions start to be discernible. This transitional belt, that occupies about 0.37 km², was classified as mosaic of Coralligenous and *Posidonia*. The visual analysis of the ROV-video transects, used as ground truth, suggests that in this zone bioconstructions, which predominantly belong to the banks morphotype develop on a hard substrate that marks a widespread break in slope all throughout the study area. This break marks the end of the transition zone, characterized by the simultaneous presence of Coralligenous and *Posidonia*.

By comparing the morphological characteristics of the seabed with the alignment of the emerged marine terraces, the presence of an additional submerged terraced surface becomes evident. It could represent a submerged portion of the 5th order terrace, currently exposed only in the Le Castella area. The submersion of this portion of the terrace in the study area would be justified by the presence of a tectonic feature with extensional kinematics, located approximately along the coastline, which, in this area, shows a distinctly straight alignment with a N-S orientation. Further studies, focusing on the geological characterization of the substrate on which coralligenous banks developed and the correlation of these lithotypes with those outcropping on land, could confirm this hypothesis.

Deeper than 25 m, upon close MBES data and ROV inspection, *Posidonia* disappears and the predominant benthic habitat is represented by Coralligenous sensu stricto. Bioconstructions, often associated with fine to medium sediment and maerl, predominantly belong to the morphotype of discrete reliefs. Bioconstructions tend to align sub-parallel to the shoreline. This distribution is associated with the presence of relatively pronounced seafloor structures, as revealed by ROV-video transects. This observation might suggest: i) a significant control of hydrodynamic conditions on the formation, development and distribution of coralligenous build-ups, or ii) an overprint of the bioconstructions on a seafloor already sculpted by the evolution of the bottom during glacial/interglacial cycles. However, further investigation is needed,

including bottom current monitoring using appropriate instruments (e.g., current meter), in order to better define these bedforms.

The benthic habitat distribution identified in the study area exhibits a clear spatial zonation, which appear to be influenced by both substrate characteristics and geomorphological features. In the shallowest sector (above -15m depth), *Posidonia oceanica* represent the prevalent benthic habitat. In the intermediate depth range (down to approximately -25m depth), a mosaic of *Posidonia* and coralligenous bioconstructions develops, indicating a transitional zone where environmental conditions allow the coexistence of seagrass and algal reefs.

Comparison between the morphological characteristics of the seabed with the alignment and elevation of the emerged marine terraces highlights the presence of a flat, laterally continuous submerged surface, as typically observed in relict marine terraces (e.g., Savini et al., 2021; Lebrech et al., 2022). This sub-horizontal platform is bounded seaward by a break in slope, located at approximately -15 m depth, interpreted as the outer margin of the terrace. Based on these evidences, the submerged surface can be correlated with the 5th order terrace exposed near Le Castella, characterized by a gently seaward-inclined surface and a morphological step interpreted as paleoclipf (Bracchi et al., 2016). The different orientation of the submerged scarp in the study area (NE-SW), compared to the emerged paleoclipf associated with Le Castella marine terrace (NW-SE to E-W), may be reasonably attributed to local coastal curvature and/or tectonic influences. The submersion of this portion of the 5th order terrace in the study area would be justified by the possible presence of a tectonic feature with extensional kinematics located approximately along the coastline, which shows a distinctly straight alignment with a N-S orientation. However, further investigations are needed to confirm this hypothesis.

The inner portion of the submerged surface is characterized by the presence of sub-spherical blocks, often colonized by *Posidonia oceanica*, which possibly result from gravitational processes affecting the adjacent 4th order marine terrace located upslope. This interpretation is supported by their rounded morphology, typically associated with detachment and downslope transport, and by the presence of scarps in the emerged portion of the study area, which could indicate past gravitational instability.

The outer portion and the edge of the submerged platform (down to approximately -25m) hosts several coralligenous build-ups, predominantly belonging to banks morphotype. Similar spatial arrangements have been observed in submerged terraces of southeastern Sicily (Varzi et al., 2022) and on wave-cut ravinement surfaces associated with fossil marine terraces, such as the mid-Pleistocene Cutro terrace (Nalin et al., 2006) and the emerged 5th order terrace of Le Castella (Bracchi et al., 2016).

In the deeper sector of the study area (below -25m depth), *Posidonia* is no longer present and the benthic assemblages are composed by Coralligenous *sensu stricto* associated with fine to medium sediments and maerl. These bioconstructions mainly belong to discrete reliefs morphotype and tend to follow a sub-parallel orientation relative to the shoreline, a distribution pattern that appears associated with relatively pronounced seafloor structures (as revealed by ROV-video transects). This spatial configuration suggests that environmental or geomorphological factors may influence the development and positioning of build-ups. Particularly, two hypotheses are proposed to explain this pattern: i) the influence of bottom currents and internal waves, which may promote the alignment of coralligenous bioconstructions, as observed in mesophotic carbonate systems of the Maltese shelf by Bialik et al. (2024); ii) an overprint of the build-ups onto inherited seabed morphologies, shaped by sea-level fluctuation and regional uplift during the Quaternary glacial/interglacial cycles, as documented on submerged terraces offshore Marzamemi (SE Sicily) by Varzi et al. (2022). However, further investigations, including in situ hydrodynamic and sediment transport measurements, are necessary to validate these hypotheses.

5.2 TPI-based feature extraction

Coralligenous build-ups were treated as distinct features in both two- and three-dimensional spaces, with the aim of using a geomorphometric parameters for their extraction from the seafloor. Variability of coralligenous morphotypes (Bracchi et al., 2017) poses several challenges to their automated extraction from DTM. Since build-ups raise from the surrounding seafloor, their detection could be performed by slope analysis. However, while slope proves effective for accurately segmenting isolated small-scale features (Savini et al., 2014; Bargain et al., 2017), it struggles to incorporate the inner areas of banks into the segmentation process. The high 3D complexity in these areas makes it challenging to create a continuous polygon. On the other hand, geomorphometric parameters like the rugosity index (i.e., TRI; Riley et al., 1999) are more successful in defining the overall distribution of bank morphotypes, but they fail to provide an accurate estimation of the size of discrete reliefs. Therefore, as noted by Marchese et al. (2020), TPI offers a good compromise for detecting coralligenous morphotypes. Indeed, it assesses the relative topographic position of a central point by calculating the difference between its elevation and the average elevation within a predefined neighbourhood. In this work, the input parameters for the calculation of the TPI have been refined in order to minimize the artifacts during the extraction process. Specifically, the choice of a threshold value of 0.2 (lower than 0.3 used by Marchese et al., 2020), combined with higher values of Power and Bandwidth compared to the default ones, has allowed for a 15% reduction in the artifact percentage compared to Marchese et al. (2020). These adjustments have therefore significantly reduced the manual review time, improving the automatization of the extraction process.

The threshold value adopted for the TPI analysis was defined through a trial-and-error procedure, as described in the methodological section. In particular, threshold values lower than 0.2 increased the morphological adherence of the extracted features to seabed forms, but at cost of a higher number of false positives (especially in areas covered by *Posidonia oceanica*, where slight topographic variations were incorrectly interpreted as relevant morphotypes). Conversely, threshold values higher than 0.2 reduced the occurrence of artifacts but led to the omission of low-relief structures, thus compromising the completeness of mapping. In this work, a threshold value of 0.2 proved to be an effective compromise, ensuring a satisfactory balance between the accuracy of morphotype extraction and the minimization of false positive. This configuration allowed for the preservation of relevant coralligenous bioconstructions, including low-relief build-ups, while significantly limiting the occurrence of artifacts.

The proposed approach, although developed only for a specific coastal area, can be transferred to other regions, provided that adequate calibration is performed. The effectiveness of TPI-based extraction depends on several factors, and no universally applicable threshold value exists, as it must be adapted to the resolution and quality of bathymetric data, as well as to the site-specific geomorphological and geobiological variability. To date, no standardized procedure is available for determining the optimal threshold; however, its selection can be refined through iterative testing supported by ground-thrut validation. Once the appropriate input parameter for TPI calculation (e.g., Power, Bandwidth, minimum and maximum radius) ad a suitable threshold value are identified, the method allows for the extraction of morphologically distinct features, provided these are sufficiently expressed relative to the surrounding seafloor.

5.3. Morphological development of coralligenous build-ups

Computation of maximum diameter, surface and volume for each build-up were performed using vector field operation in QGIS. Quantitative morphometric data extracted from the proposed benthic habitat model were plotted in the scatterplots of Figure 8. The quantitative morphometric data (i.e., surface, thickness, volume, maximum diameter and shape indices), extracted from the benthic habitat mapping model proposed in this work, were plotted in the scatterplots

of Figure 8, providing new insights into spatial distribution, morphotype variability and growth pattern of the coralligenous build-ups across the study area.

Most polygons, representing aggregates of different coralligenous build-ups, are characterized by areas smaller than 200 m² and less than 1 m thick (Fig. 8A). However, discrete reliefs and banks display some differences in their distribution: discrete reliefs tend to cluster in the lower part of the graph (smaller areas and lower thickness), whereas banks with similar thickness generally exhibit larger areas on average.

The volume of the build-ups is strongly dependent on thickness, suggesting that vertical growth plays a key role in the formation of these structures (Fig. 8B). However, discrete reliefs show a more irregular distribution, with a greater dispersion of data ($R^2= 0.36$ 0.35). This trend suggests that volume increase depends not only on thickness but also on a significant lateral growth component. Conversely, banks exhibit a more regular trend, with volume increasing proportionally with thickness. The strong correlation between thickness and volume ($R^2= 0.83$) aligns with a growth pattern that is almost exclusively vertical for this morphotype.

The relationships between area and shape indices (SI) of coralligenous build-ups (Fig. 8C), despite a moderate data dispersion, revealed a positive correlation ($R^2=0.61$), suggesting that more irregularly shaped bioconstructions (typically associated with the morphotypes of banks) tend to cover larger areas. Moreover, banks also tend to have larger maximum diameter (Dmax), as suggested by an R^2 value of 0.78 (Fig. 8D). However, the greater variability in area might reflect higher spatial complexity in the distribution of these structures.

The relationship between depth and thickness of coralligenous bioconstructions, divided into banks (Fig. 8F) and discrete reliefs (Fig. 8E), reveals that both morphotypes exhibit average decreasing thickness with increasing depth. However, discrete reliefs show greater thickness variability, with higher dispersion of data at depths shallower than -25 m, whereas for the banks, data distribution is more regular. The decrease in the thickness of bioconstructions with increasing depth could be attributed to various causes, including changes in hydrodynamic energy, the characteristics of the substrate on which the bioconstructions develop, or sedimentation conditions.

To date, no previous study has provided morphometric analysis of coralligenous build-ups based on quantitative extraction of 2D/3D parameters (e.g., area, thickness, volume, shape indices) from high-resolution MBES data. Therefore, a direct comparison of our results with other Mediterranean coralligenous fields is currently not possible. Nonetheless, several works have described the geomorphological variability of coralligenous morphotypes across the Mediterranean basin (e.g., Bracchi et al., 2015, 2017, 2022; Marchese et al., 2020). These studies recognize the coexistence of morphotypes such as banks and discrete reliefs, often occurring over short spatial scale and associated with different environmental conditions. The same spatial mixing of these morphotypes, which may be due to small-scale variations in substrate type, hydrodynamic regime, or inherited seabed features, which locally favour distinct growth mode despite spatial proximity (Bracchi et al., 2017; Marchese et al., 2020; Varzi et al., 2022), was also observed in our study area.

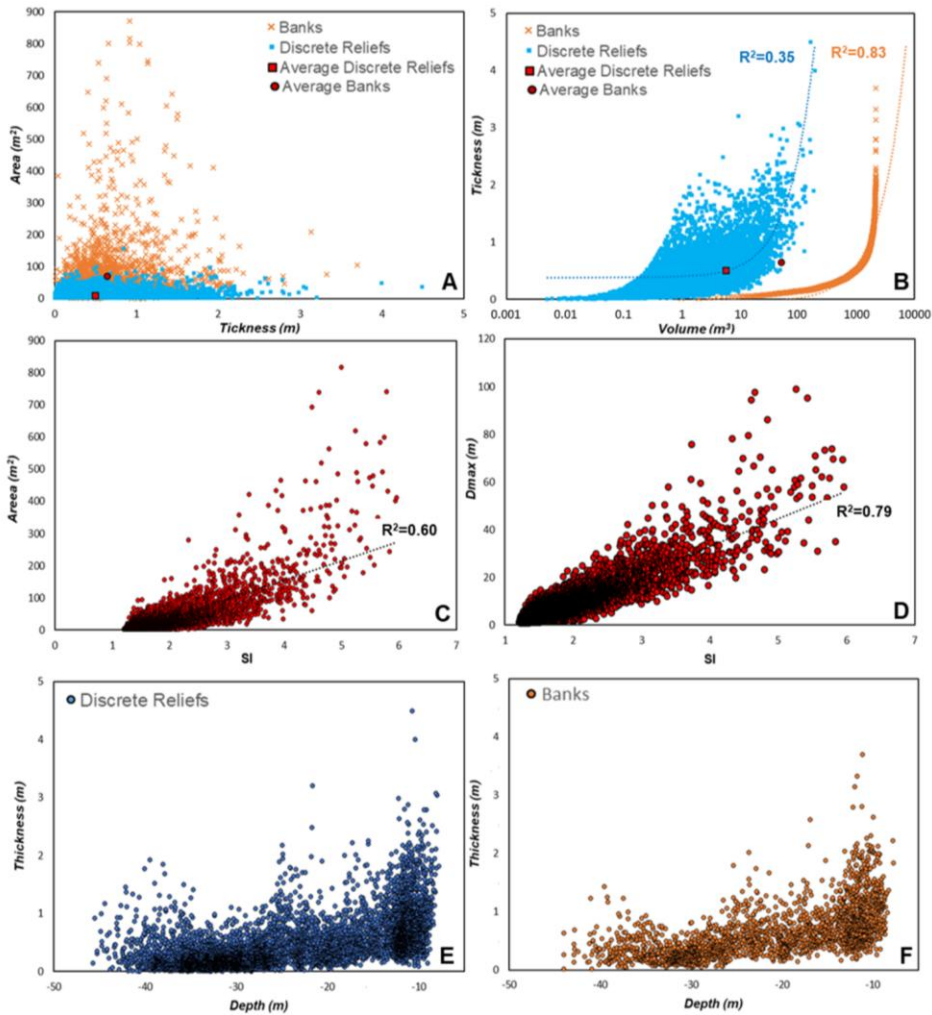


Figure 8: Scatterplot representing relationships between: area and thickness (A); thickness and volume (B); area and shape index (C); maximum diameter and shape index (D); thickness and depth for banks (E) and discrete relief (F). These quantitative geometric data were extracted by the benthic habitat mapping model proposed in this work. SI: shape index; Dmax: maximum diameter.

CONCLUSIONS

A new mapping protocol approach starting from high-resolution acoustic data acquired through MBES surveys performed offshore Capo Bianco (Isola Capo Rizzuto Marine Protected Area) was developed and presented here. The method protocol represents a step forward, as it builds on an integrated two foundational approaches in coralligenous habitat studies: the morphotyping of Coralligenous based on the shape index, and their spatial and volumetric quantification. The innovation of this work lies in the synthesis of these methodologies, which were applied and refined in a new study area. Moreover, the approach protocol, which integrates bathymetric and backscatter data with geomorphological and

geomorphometric indices, was performed using open-source software, providing a detailed workflow that can be freely reproduced and adopted by organizations involved in research, monitoring and conservation of marine habitats. The resulting model proved capable not only in identifying and differentiating the benthic habitats but also in providing new quantitative information regarding the spatial distribution and 2D/3D geometric characteristics of the extracted coralligenous build-ups. This innovative aspect, compared to the traditional mapping protocol, is crucial for the quantification of the structural complexity of these bioconstructions. Moreover, this approach enables monitoring of variations not only in terms of the habitat's areal extent, but also in terms of vertical development of Coralligenous relative to the substrate from which build-ups form. Indeed, the quantitative geomorphometric data obtained from the mapping model of Capo Bianco seafloor were analyzed, revealing significant insights into the covered surface, volume and thickness of build-ups, as well as the relationships among these parameters. In particular, the results highlighted that the discrete reliefs morphotype exhibit a much more pronounced lateral growth component compared to the banks. If confirmed through an accurate geobiological characterization, these finding could provide important new insights about the tempo and mode of the inception and development of these hard-biogenic substrates, crucial for the conservation of Mediterranean biodiversity.

Author contributions

Conceptualization: G.M., A.G.; Methodology: G.M., A.G., G.I., F.M.; Formal analysis and investigation: G.M., M.C., G.I.; U.S.; F.M.; Writing – original draft preparation: G.M., M.C., G.V., F.P., A.L., E.C., R.S.; Writing – review and editing: R.D., C.A., F.B., V.A.B., D.B., A.R., A.G.; Funding acquisition: A.G., F.B.; Resources: R.D., F.B., A.L., E.C., A.G.; Supervision: A.G.

Competing interests

The contact author has declared that none of the authors has any competing interests.

Acknowledgments

We would like to express our sincere gratitude to the Geobiology and Marine Laboratories of the DiBEST, University of Calabria, for their invaluable support and contribution to this work.

Financial support

This work was funded by the Next Generation EU – Tech4You – “Technologies for climate change adaptation and quality of life improvement – Tech4You”, Project “Development of tools and applications for integrated marine communities and substrates monitoring”, PP 2.3.1 – Action 1 “Development of hardware and software systems for three-dimensional detection, sampling and mapping of underwater environments”, CUP H23C22000370006. This work reflects only the authors' views and opinions, neither the Ministry for University and Research nor the European Commission can be considered responsible for them.

Open Research

The data sets needed to evaluate results and conclusion in this paper are available at http://geocube.unical.it/gmaruca/Dataset_Benthic_Habitat_Mapping.zip (Maruca et al., 2025). The raw data used in this study were acquired through MBES survey using a pole-mounted, Norbit WBMS Basic multibeam sonar system

integrated with GNSS/INS (Applanix OceanMaster). The processing of MBES bathymetric data was performed using QPS Qimera (<https://qps.nl/qimera/>). Backscatter data processing was performed using QPS Fledermaus (<https://qps.nl/fledermaus/>). Figures 1, 3, 4, 6, 7 were made with QGIS 3.34.9 “Prizren” software (<https://qgis.org/project/overview/>). Figures 8 were generated using Microsoft Excel (<https://www.microsoft.com/it-it/microsoft-365>). Data used to generate the figures are available upon request to the corresponding author.

REFERENCES

- Abdullah, M. Z., Chuah, L.F., Zakariya, R., Syed, A., Rozaimi, C. H., Mahmud, S. M., Abdallah M. E., Bokhari, A., Muhammad, S. A. and Al-Shwaiman, H. A.: Evaluating climate change impacts on reef environments via multibeam echosounder and Acoustic Doppler Current profiler technology. *Environmental Research*, Volume 252, Part 3, 118858, <https://doi.org/10.1016/j.envres.2024.118858>, 2024.
- Arosio, R., Hobley, B., Wheeler, A. J., Sacchetti, F., Conti, L. A., Furey, T. and Lim, A.: Fully convolutional neural networks applied to large-scale marine morphology mapping. *Frontiers in Marine Science*, 10-1228967, <https://doi.org/10.3389/fmars.2023.1228967>, 2023.
- Ballesteros, E.: Mediterranean Coralligenous Assemblages: a synthesis of present knowledge. *Oceanography and Marine Biology*, Annual Review, 44, 123–195, 2006.
- Basso, D., Bracchi, V. A., Bazzicalupo, P., Martini, M., Maspero, F. and Bavestrello, G.: Living coralligenous as geo-historical structure built by coralline algae. *Frontiers in Earth Science*, 10, 961632, <https://doi.org/10.3389/feart.2022.961632>, 2022.
- Bazzicalupo, P., Cipriani, M., Guido, A., Bracchi, V. A., Rosso, A. and Basso, D.: Calcareous nannoplankton inside coralligenous build-ups: the case of Marzamemi (SE, Sicily). *Bollettino della Società Paleontologica Italiana*, 63 (1), 89–99, <https://dx.doi.org/10.4435/BSPI.2024.09>, 2024.
- Belluomini, G., Gliozzi, E., Ruggieri, G., Branca, M. and Delitala, L.: First dates on the terraces of the Cortone Peninsula (Calabria, southern Italy). *Italian Journal of Geosciences*, 107 (1), 249–254, 1988.
- Betzler, C., Brachert, T. C., Braga, J. C. and Martin, J. M.: Nearshore, temperate, carbonate depositional systems (lower Tortonian, Agua Amarga Basin, southern Spain): Implications for carbonate sequence stratigraphy. *Sedimentary Feology*, 113, 27–53, 1977.
- Bishop, M. P., James, L. A., Shroder, J. F. & Walsh, S. J.: Geospatial technologies and digital geomorphological mapping: Concepts, issues and research. *Geomorphology*, 137, 5–26, <http://dx.doi.org/10.1016/j.geomorph.2011.06.027>, 2012.
- Bonardi, G., Cavazza, W., Perrone, V. and Rossi, S.: Calabria–Peloritani terrane and northern Ionian Sea. In Vai, G. B. & Martini, I. P. (eds.), *Anatomy of an Orogen: The Apennines and Adjacent Mediterranean Basins*, Kluwer Academic Publishers (pp. 287–306), http://dx.doi.org/10.1007/978-94-015-9829-3_17, 2001.

647 Bracchi, V. A., Basso, D., Marchese, F., Corselli, C. and Savini, A.: Coralligenous morphotypes on subhorizontal
648 substrate: A new categorization. *Continental Shelf Research*, 144, 10–20. <http://dx.doi.org/10.1016/j.csr.2017.06.005>,
649 2017.

650

651 Bracchi, V. A., Bazzicalupo, P., Fallati, L., Varzi, A. G., Savini, A., Negri, M. P., Rosso, A., Sanfilippo, R., Guido, A.,
652 Bertolino, M., Costa, G., De Ponti, E., Leonardi, R., Muzzupappa, M., and Basso, D.: The Main Builders of Mediterranean
653 Coralligenous: 2D and 3D Quantitative Approaches for its Identification. *Frontiers in Earth Science*, 10, 910522
654 <https://doi.org/10.3389/feart.2022.910522>, 2022.

655

656 Bracchi, V. A., Nalin, R. and Basso D.: Morpho-structural heterogeneity of shallow–water coralligenous in a Pleistocene
657 marine terrace (Le Castella, Italy). *Palaeogeography, Palaeoclimatology, Palaeoecology*, 454, 101–112,
658 <http://dx.doi.org/10.1016/j.palaeo.2016.04.014>, 2016.

659

660 Bracchi, V. A., Nalin, R. and Basso, D.: Paleoeecology and dynamics of coralline–dominated facies during a Pleistocene
661 transgressive–regressive cycle (Capo Colonna marine terrace, Southern Italy). *Palaeogeography, Palaeoclimatology,*
662 *Palaeoecology*, 414, 296–309, <http://dx.doi.org/10.1016/j.palaeo.2014.09.016>, 2014.

663

664 Bracchi, V. A., Savini, A., Marchese, F., Palamara, S., Basso, D. and Corselli C.: Coralligenous habitat in the
665 Mediterranean Sea: a geomorphological description from remote data. *Italian Journal Geosciences*, 134 (1), 32–40,
666 <https://doi.org/10.3301/IJG.2014.16>, 2015.

667

668 Brown, C. J., Sameoto, J. A., & Smith, S. J.: Multiple methods, maps, and management applications: Purpose made
669 seafloor maps in support of ocean management. *Journal of Sea Research*, 72, 1–13,
670 <https://doi.org/10.1016/j.seares.2012.04.009>, 2012.

671

672 Cavazza, W., Blenkinsop, J., De Celles, P. G., Patterson, R. T. and Reinhardt, E. G.: Stratigrafia e sedimentologia della
673 sequenza sedimentaria oligocenica–quaternaria del bacino Calabro–Ionico. *Bollettino della Società Paleontologica*
674 *Italiana*, 116, 51–77, 1997.

675

676 Chiocci, F. L., Budillon, F., Ceramicola, S., Gamberi, F. and Orrù, P.: Atlante dei lineamenti di pericolosità geologica dei
677 mari italiani. CNR edizioni, RM: Risultati del progetto MaGIC, 2021.

678

679 Cipriani, M., Apollaro, C., Basso, D., Bazzicalupo, P., Bertolino, M., Bracchi, V. A., Bruno, F., Costa, G., Dominici, R.,
680 Gallo, A., Muzzupappa, M., Rosso, A., Sanfilippo, S., Sciuto, F., Vespasiano, G. and Guido, A.: Origin and role of non–
681 skeletal carbonate in coralligenous build–ups: new geobiological perspectives in biomineralization processes.
682 *Biogeosciences*, 21, 49–72, <https://doi.org/10.5194/bg-21-49-2024>, 2024.

683

684 Cipriani, M., Basso, D., Bazzicalupo, P., Bertolino, M., Bracchi, V. A., Bruno, F., Costa, G., Dominici, R., Gallo, A.,
685 Muzzupappa, M., Rosso, A., Perri, F., Sanfilippo, R., Sciuto, F. and Guido, A.: The role of non–skeletal carbonate
686 component in Mediterranean Coralligenous: new insight from the CRESCIBLUREEF project. *Rendiconti Online Società*
687 *Geologica Italiana*, 59, 75–79. <https://doi.org/10.3301/ROL.2023.12>, 2023.

688 Conrad, O., Bechtel, B., Bock, M., Dietrich, H., Fischer, E., Gerlitz, L., Wehberg, J., Wichmann, V. and Bohner, J.:
 689 System for Automated Geoscientific Analyses (SAGA). Geoscientific model development, 8,
 690 <https://doi.org/10.5194/gmd-8-1991-2015>, 2015.
 691
 692 Cosentino, D., Gliozzi, E. and Salvini, F.: Brittle deformations in the Upper Pleistocene deposits of the Crotona Peninsula,
 693 Calabria, southern Italy. Tectonophysics, 163, 205–217, 1989.
 694
 695 Cutter, G. R., Rzhano, Y. and Mayer, L. A.: Automated segmentation of seafloor bathymetry from multibeam
 696 echosounder data using local fourier histogram texture features. Journal of Experimental Marine Biology and Ecology,
 697 285, 355–370. [http://dx.doi.org/10.1016/S0022-0981\(02\)00537-3](http://dx.doi.org/10.1016/S0022-0981(02)00537-3), 2003.
 698
 699 De Falco, G., Conforti, A., Brambilla, W., Budillon, F., Ceccherelli, G. and De Luca, M.: Coralligenous banks along the
 700 western and northern continental shelf of Sardinia Island (Mediterranean Sea). Journal of Maps, 18(2), 200–209.
 701 <https://doi.org/10.1080/17445647.2021.2020179>, 2022.
 702
 703 De Falco, G., Tonielli, R., Di Martino, G., Innangi, S., Simeone, S. and Parnum, I. M.: Relationships between multibeam
 704 backscatter, sediment grain size and Posidonia oceanica seagrass distribution. Continental Shelf Research, 30(18), 1941–
 705 1950. <https://doi.org/10.1016/j.csr.2010.09.006>, 2010.
 706
 707 Deias, C., Guido, A., Sanfilippo, R., Apollaro, C., Dominici, R., Cipriani, M., Barca, D., and Vespasiano, G.: Elemental
 708 Fractionation in Sabellariidae (Polychaeta) Biocement and Comparison with Seawater Pattern: A New Environmental
 709 Proxy in a High–Biodiversity Ecosystem? Water, 15, 1549, <https://doi.org/10.3390/w15081549>, 2023.
 710
 711 Di Geronimo, I., Di Geronimo, R., Improta, S., Rosso, A. and Sanfilippo, R.: Preliminary observation on a columnar
 712 coralline build-up from off SE Sicily. Biologia Marina Mediterranea, 8(1), 229–237, 2001.
 713
 714 Donato, G., Sanfilippo, R., Basso, D., Bazzicalupo, P., Bertolino, M., Bracchi, V. A., Cipriani, M., D’Alpa, F., Guido,
 715 A., Negri, M. P., Sciuto, F., Serio, D. and Rosso, A.: Biodiversity associated with a coralligenous build-up off Sicily
 716 (Ionian Sea). Regional Studies in Marine Science, 80, 103868, <https://doi.org/10.1016/j.rsma.2024.103868>, 2024.
 717
 718 Faccenna, C., Becker, T. W., Lucente, F. P., Jolivet, L. and Rossetti, F.: History of subduction and back-arc extension in
 719 the Central Mediterranean. Geophysical Journal International, 145 (3), 809–820. <http://dx.doi.org/10.1046/j.0956-540x.2001.01435>, 2001.
 720
 721 Faccenna, C., Molin, P., Orecchio, B., Olivetti, V., Bellier, O., Funicello, F., Minelli, L., Piromallo, C. and Billi, A.:
 722 Topography of the Calabria subduction zone (Southern Italy): clues for the origin of Mt. Etna. Tectonics, 30, TC1003.
 723 <http://dx.doi.org/10.1029/2010TC002694>. 2011.
 724
 725 Fakiris, E. and Papatheodorou, G.: Quantification of regions of interest in swath sonar backscatter images using grey-
 726 level and shape geometry descriptors: The TargAn software. Marine Geophysical Research, 33, 169–183,
 727 <http://dx.doi.org/10.1007/s11001-012-9153-5>, 2012.
 728

729 Ferrigno, F., Rendina, F., Sandulli, R. and Fulvio Russo, G.: Coralligenous assemblages: research status and trends of a
730 key Mediterranean biodiversity hotspot through bibliometric analysis. *Ecological Questions* 35, 1: 19-36,
731 <http://dx.doi.org/10.12775/EQ.2024.001>, 2024.

732

733 Foglini, F., Grande, V., Marchese, F., Bracchi, V. A., Prampolini, M., Angeletti, L., Castellan, G., Chimienti, G., Hansen,
734 I. M., Gudmundsen, M., Meroni, A. N., Mercorella, A., Vertino, A., Badalamenti, F., Corselli, C., Erdal, I., Martorelli,
735 E., Savini, A. and Taviani, M.: Application of Hyperspectral Imaging to Underwater Habitat Mapping, Southern Adriatic
736 Sea. *Sensors*, 19, 2261, <https://doi.org/10.3390/s19102261>, 2019.

737

738 Fonseca, L., and Mayer, L.: Remote estimation of surficial seafloor properties through the application of angular range
739 analysis to multibeam sonar data. *Marine Geophysical Research*, 28, 119–126, [https://doi.org/10.1007/s11001-007-9019-](https://doi.org/10.1007/s11001-007-9019-4)
740 [4](https://doi.org/10.1007/s11001-007-9019-4), 2007.

741

742 Garone, R.V., Lønmo, T., I., B., Schimel, A. C. G., Diesing, M., Thorsnes, T. and Løvstakken, L.: Seabed classification
743 of multibeam echosounder data into bedrock/non-bedrock using deep learning. *Frontiers in Earth Science*, 11:1285368,
744 <https://doi.org/10.3389/feart.2023.1285368>, 2023.

745

746 Gerovasileiou V. and Bianchi, C. N.: Mediterranean marine caves: a synthesis of current knowledge. In S. J. Hawkins,
747 A. J. Lemasson, A. L. Allcock, A. E. Bates, M. Byrne, A. J. Evans, L. B. Firth, E. M. Marzinelli, B. D. Russell, I. P.
748 Smith, S. E. Swearer, P. A. (Eds.), *Oceanography and Marine Biology: An Annual Review*, (Vol. 59, pp. 1–88). Todd,
749 Editors Taylor & Francis, <https://doi.org/10.1201/9781003138846-1>, 2021.

750

751 Gliozzi, E.: I terrazzi marini del Pleistocene superiore della penisola di Crotone (Calabria). *Geologica Romana*, 26, 17–
752 79, 1987.

753

754 Guido, A., Gerovasileiou, V., Russo, F., Rosso, A., Sanfilippo, R., Voultsiadou, E. and Mastandrea, A.: Composition and
755 biostratigraphy of sponge-rich biogenic crusts in submarine caves (Aegean Sea, Eastern Mediterranean). *Palaeogeography,*
756 *Palaeoclimatology, Palaeoecology*, 534, 109338, <https://doi.org/10.1016/j.palaeo.2019.109338>, 2019a.

757

758 Guido, A., Gerovasileiou, V., Russo, F., Rosso, A., Sanfilippo, R., Voultsiadou, E. and Mastandrea, A.: Dataset of
759 biogenic crusts from submarine caves of the Aegean Sea: An example of sponges vs microbialites competitions in cryptic
760 environments.” *Data in brief*, 27, 104745, <https://doi.org/10.1016/j.dib.2019.104745>, 2019b.

761

762 Guido, A., Heindel, K., Birgel, D., Rosso, A., Mastandrea, A., Sanfilippo, R., Russo, F. and Peckmann, J.: Pendant
763 bioconstructions cemented by microbial carbonate in submerged marine cave (Holocene, SE Sicily). *Palaeogeography,*
764 *Palaeoclimatology, Palaeoecology*, 388, 166–180. <http://dx.doi.org/10.1016/j.palaeo.2013.08.007>, 2013.

765

766 Guido, A., Jimenez, C., Achilleos, K., Rosso, A., Sanfilippo, R., Hadjioannou, L., Petrou, A., Russo, F. and Mastandrea,
767 A.: Cryptic serpulid-microbialite bioconstructions in the Kakoskali submarine cave (Cyprus, Eastern Mediterranean).
768 *Facies*, 63(21), <http://dx.doi.org/10.1007/s10347-017-0502-3>, 2017b.

Guido, A., Rosso, A., Sanfilippo, R., Miriello, D. and Belmonte, G.: Skeletal vs microbialite geobiological role in bioconstructions of confined marine environments. *Palaeogeography, Palaeoclimatology, Palaeoecology*, 593, 110920, <https://doi.org/10.1016/j.palaeo.2022.110920>, 2022.

Guido, A., Rosso, A., Sanfilippo, R., Russo, F. and Mastandrea, A.: Frutexitites from microbial/metazoan bioconstructions of recent and Pleistocene marine caves (Sicily, Italy). *Palaeogeography, Palaeoclimatology, Palaeoecology*, 453, 127–138. <http://dx.doi.org/10.1016/j.palaeo.2016.04.025>, 2016.

Guido, A., Rosso, A., Sanfilippo, R., Russo, F. and Mastandrea, A.: Microbial Biomineralization in Biotic Crusts from a Pleistocene Marine Cave (NW Sicily, Italy).” *Geomicrobiology Journal*, 34 (10), 864–872, <https://doi.org/10.1080/01490451.2017.1284283>, 2017a.

Ingrosso, G., Abbiati, M., Badalamenti, F., Bavestrello, G., Belmonte, G., Cannas, R., Benedetti Cecchi, L., Bertolino, M., Bevilacqua, S., Bianchi, C. N., Bo, M., Boscari, E., Cardone, F., Cattaneo Vietti, R., Cau, A., Cerrano, C., Chemello, R., Chimienti, G., Congiu, L., Corriero, G., Costantini, F., De Leo, F., Donnarumma, L., Falace, A., Fraschetti, S., Giangrande, A., Gravina, M.F., Guarnieri, G., Mastrototaro, F., Milazzo, M., Morri, C., Musco, L., Pezzolesi, L., Piraino, S., Prada, F., Ponti, M., Rindi, F., Russo, G.F., Sandulli, R., Villamor, A., Zane, L. and Boero, F.: Mediterranean Bioconstructions Along the Italian Coast. *Advances in Marine Biology*, 79:61-136, <https://doi.org/10.1016/bs.amb.2018.05.001>, 2018.

Innangi, S., Barra, M., Di Martino, G., Parnum, I. M., Tonielli, R. and Mazzola, S.: Reson SeaBat 8125 backscatter data as a tool for seabed characterization (Central Mediterranean, Southern Italy): Results from different processing approaches. *Applied Acoustics*, 87, 109–122, <https://doi.org/10.1016/j.apacoust.2014.06.014>, 2015.

Innangi, S., Ferraro, L., Innangi, M., Di Martino, G., Giordano, L., Bracchi, V.A. and Tonielli, R.: Linosa island: a unique heritage of Mediterranean biodiversity. *Journal of Maps*, 20(1), 2297989, <https://doi.org/10.1080/17445647.2023.2297989>, 2024.

Ismail, K., Huvenne, V. A. I. and Masson, D. G.: Objective automated classification technique for marine landscape mapping in submarine canyons. *Marine Geology*, 362, 17–32, <https://doi.org/10.1016/j.margeo.2015.01.006>, 2015.

Janowski, L., Trzcinska, K., Tegowski, J., Kruss, A., Rucinska-Zjadacz, M. and Pocwiardowski P.: Nearshore Benthic Habitat Mapping Based on Multi-Frequency, Multibeam Echosounder Data Using a Combined Object-Based Approach: A Case Study from the Rowy Site in the Southern Baltic Sea. *Remote Sensing*, 10, 1983, <https://doi.org/10.3390/rs10121983>, 2018.

Jardim, V.L., Grall, J., Barros-Barreto, M.B., Bizien, A., Benoit, T., Braga, J.C., Brodie, J., Burel, T., Cabrito, A., Diaz-Pulido, G., Gagnon, P., Hall-Spencer, J.M., Helias, M., Horta, P.A., Joshi, S., Kamenos, N.A., Kolzenburg, R., Krieger, E.C., Legrand, E., Page, T.M., Peña, V., Ragazzola, F., Rasmussen, L.M., Rendina, F., Schubert, N., Silva, J., Tâmega, F.T.S., Tauran, A. and Burdett, H.L.: A Common Terminology to Unify Research and Conservation of Coralline Algae and the Habitats They Create. *Aquatic Conservation: Marine and Freshwater Ecosystems*. 35: e70121, <https://doi.org/10.1002/aqc.70121>, 2025.

811 Laborel, J.: Marine biogenic constructions in the Mediterranean. A review. Scientific Reports of Port-Cros National Park
812 13, 97–126, 1987.

813

814 Lurton, X. Lamarche, G., Brown, C., Lucieer, V., Rice, G., Schimel, A. and Weber, T. (Eds): Backscatter Measurements
815 by Seafloor-mapping Sonars. Guidelines and Recommendations. GeoHab, 200p,
816 <https://doi.org/10.5281/zenodo.10089261>, 2015.

817

818 Lamarche G. and Lurton X.: Recommendations for improved and coherent acquisition and processing of backscatter data
819 from seafloor-mapping sonars. Marine Geophysical Research, 39:5-22, <https://doi.org/10.1007/s11001-017-9315-6>,
820 2018.

821

822 Lebrech, U., Riera, R., Paumard, V., Leary, M. J. O. and Lang, S. C.: Morphology and distribution of Submerged
823 palaeoshorelines: Insights from the North West Shelf of Australia. Earth-Science Reviews, 224, 103864,
824 <https://doi.org/10.1016/j.earscirev.2021.103864>, 2022.

825

826 Lecours, V., Devillers, R., Schneider, D. C., Lucieer, V. L., Brown, C. J., and Edinger, E. N.: Spatial scale and geographic
827 context in benthic habitat mapping: Review and future directions. Marine Ecology Progress Series, 535, 259–284,
828 <https://doi.org/10.3354/meps11378>, 2015.

829

830 Lecours, V., Dolan, M. F. J., Micallef, A. and Lucieer, V. L.: A review of marine geomorphometry, the quantitative study
831 of the seafloor. Hydrology and Earth System Sciences, 20, 3207–3244, <https://doi.org/10.5194/hess-20-3207-2016>, 2016.

832 Lo Iacono, C., Savini, A. and Basso, D.: Cold-Water carbonate bioconstructions. In Micallef A., Krastel S. & Savini A.
833 (Eds.) Submarine geomorphology, (pp. 425–455). Springer, ISBN: 425-3-319-57851-4, https://doi.org/10.1007/978-3-319-57852-1_22, 2018.

834

835

836 Lucieer, V. and Lamarche, G.: Unsupervised fuzzy classification and object-based image analysis of multibeam data to
837 map deep water substrates, Cook Strait, New Zealand. Continental Shelf Research, 31, 1236–1247.
838 <https://doi.org/10.1016/j.csr.2011.04.016>, 2011.

839

840 Malinverno, A. and Ryan, W. B. F.: Extension in the Tyrrhenian Sea and shortening in the Apennines as result of arc
841 migration driven by sinking of the lithosphere. Tectonics, 5 (2), 227–245. <http://dx.doi.org/10.1029/TC005i002p00227>,
842 1986.

843

844 Marchese, F., Bracchi, V. A., Lisi, G., Basso, D., Corselli, C. and Savini, S.: Assessing Fine-Scale Distribution and
845 Volume of Mediterranean Algal Reefs through Terrain Analysis of Multibeam Bathymetric Data. A Case Study in the
846 Southern Adriatic Continental Shelf, Water, 12, 157. 10.3390/w12010157, 2020.

847

848 Maruca, G., Cipriani, M., Dominici, R., Imbrogno, G., Vespasiano, G., Apollaro, C., Perri, F., Bruno, F., Lagudi, A.,
849 Severino, U., Bracchi, V. A., Basso, D., Cellini, E., Mauri, F., Rosso, A., Sanfilippo, R. and Guido, A.: Dataset Benthic
850 Habitat Mapping [data set], http://geocube.unical.it/gmaruca/Dataset_Benthic_Habitat_Mapping.zip, 2025.

Massari, F. and Prosser, G.: Late Cenozoic tectono-stratigraphic sequences of the Crotona Basin: insights on the geodynamic history of the Calabrian arc and Tyrrhenian Sea. *Basin Research*, 25, 26–51, <http://dx.doi.org/10.1111/j.1365-2117.2012.00549>, 2013.

Mauz, B. and Hassler, U.: Luminescence chronology of late Pleistocene raised beaches on Southern Italy: new data on relative sea-level changes. *Marine Geology*, 170, 187–203, [http://dx.doi.org/10.1016/S0025-3227\(00\)00074-8](http://dx.doi.org/10.1016/S0025-3227(00)00074-8), 2000.

McGarigal, K. and Marks, B. J. F.: *Spatial Pattern Analysis Program for Quantifying Landscape Structure* (General Technical Report) Washington, DC, USA, 1995.

Micallef, A., Le Bas, T.P., Huvenne, V. A. I., Blondel, P., Hühnerbach, V. and Deidun, A.: A multi-method approach for benthic habitat mapping of shallow coastal areas with high-resolution multibeam data. *Continental Shelf Research*, 39, 14–26, <https://doi.org/10.1016/j.csr.2012.03.008>, 2012.

Milia, A. and Torrente, M. M.: Early-stage rifting of the southern Tyrrhenian region: the Calabria–Sardinia breakup. *Journal of Geodynamics*, 81, 17–29, <http://dx.doi.org/10.1016/j.jog.2014.06.001>, 2014.

Minelli, L. and Faccenna, C.: Evolution of the Calabrian accretionary wedge (Central Mediterranean). *Tectonics*, 29, TC4004, <http://dx.doi.org/10.1029/2009TC002562>, 2010.

Nalin, R. and Massari, F.: Facies and stratigraphic anatomy of a temperate carbonate sequence (Capo Colonna Terrace, late Pleistocene, Southern Italy). *Journal of sedimentary research*, 79 (4), 210–225. <http://dx.doi.org/10.2110/jsr.2009.027>, 2009.

Nalin, R., Basso, D. and Massari, F.: Pleistocene coralline algal build-ups (coralligène de plateau) and associated bioclastic deposits in the sedimentary cover of Cutro marine terrace (Calabria, Southern Italy). In Pedley, H.M., Carannante, G. (Eds.), *Cool–Water Carbonates: Depositional Systems and Palaeoenvironmental Controls*. The Geological Society of London (pp.11–22), <http://dx.doi.org/10.1144/GSL.SP.2006.255.01.02>, 2006.

Nalin, R., Bracchi, V. A., Basso D. and Massari, F.: *Persististrombus latus* (Gmelin) in the upper Pleistocene deposits of the marine terraces of the Crotona peninsula (Southern Italy). *Italian Journal of Geosciences*, 131 (1), 95–101. <http://dx.doi.org/10.3301/IJG.2011.25>, 2012.

Nalin, R., Massari, F. and Zecchin, M.: Superimposed cycles of composite marine terraces: the example of Cutro Terrace (Calabria, Southern Italy). *Journal of sedimentary research*, 77, 340–354. <http://dx.doi.org/10.2110/jsr.2007.030>, 2007.

Palmentola, G., Carobene, L., Mastronuzzi, G. and Sansò, P.: I terrazzi marini pleistocenici della Penisola di Crotona (Italia). *Geografia Fisica e Dinamica Quaternaria*, 13, 75–80, 1990.

Pepe, F., Sulli, A., Bertotti, G., and Cella F.: Architecture and Neogene to Recent evolution of the western Calabrian continental margin: An upper plate perspective to the Ionian subduction system, central Mediterranean. *Tectonics*, 29, TC3007, <https://doi.org/10.1029/2009TC002599>, 2010.

893

894 Pèrès, J. M. and Picard, J. : Nouveau manuel de bionomie benthique de la Mer Méditerranée. Recent Travaux de la Station
895 Marine d'Endoume, 31 (47),137, 1964.

896

897 Pèrès, J. M.: Structure and dynamics of assemblages in the benthal. *Marine Ecology*, 5 (1),119–185, 1982.

898

899 Picone, F. and Chemello, R.: Seascape characterization of a Mediterranean vermetid reef: a structural complexity
900 assessment. *Frontiers in Marine Science*, 10, 1134385, doi:10.3389/fmars.2023.1134385, 2023.

901

902 Reitz, M. A. and Seeber, L.: Arc–parallel strain in a short rollback–subduction system: the structural evolution of the
903 Crotone basin (Northeastern Calabria, Southern Italy). *Tectonics*, 31, TC4017, <http://dx.doi.org/10.1029/2011TC003031>,
904 2012.

905

906 Riley, S. J., De Gloria, S. D. and Elliot, R.: A Terrain Ruggedness Index that Quantifies Topographic Heterogeneity.
907 *International Journal of Scientific Research*, 5, 23–27, 1999.

908

909 Rosso, A., Donato, G., Sanfilippo, R., Serio, D., Sciuto, F., D’Alpa, F., Bracchi, V.A., Negri, M.P. and Basso D.: The
910 bryozoan *Margaretta cereoides* as a habitat–former in the Coralligenous of Marzamemi (SE Sicily, Mediterranean Sea).
911 In Koulouri P., Gerovasileiou V. & Dailianis T. (Eds), *Marine Benthic Biodiversity of Eastern Mediterranean Ecosystems*,
912 *Journal of Marine Science and Engineering*, (Vol. 11, 590), <https://doi.org/10.3390/jmse11030590>, 2023.

913

914 Rueda, J.L., Urrea, J., Aguilar, R., Angeletti, L., Bo, M., García-Ruiz, C. Gonzalez-Duarte, M. M., Lopez, E., Madurell,
915 T., Maldonado, M., Mateo-Ramirez, A., Megina, C., Moreira, J., Moya, F., Ramalho, L. V., Rosso, A., Sitjà, C. and
916 Taviani, M.: Cold–Water Coral Associated Fauna in the Mediterranean Sea and Adjacent Areas. In Orejas C., Jiménez
917 C. (Eds.), *Mediterranean Cold–Water Corals: Past, Present and Future*, *Coral Reefs of the World* (Vol. 9 (29), pp. 295–
918 333) Springer International Publishing AG, part of Springer Nature, https://doi.org/10.1007/978-3-319-91608-8_29, 2019.

919

920 Sanfilippo, R., Rosso, A., Mastandrea, A., Viola, A., Deias, C. and Guido, A.: *Sabellaria alveolata* sandcastle worm from
921 the Mediterranean Sea: New insights on tube architecture and biocement. *Journal of Morphology*, 280, 1839–1849,
922 <https://doi.org/10.1002/jmor.21069>, 2019.

923

924 Sanfilippo, R., Rosso, A., Viola, A., Guido, A. and Deias, C.: Architecture and tube structure of *Sabellaria spinulosa*
925 (Leuckart, 1849): comparison with the Mediterranean *S. alveolata* congener. *Journal of Morphology*, 283, 1350–1358,
926 <https://doi.org/10.1002/jmor.21507>, 2022.

927

928 Santagati, P., Guerrieri, S., Borrelli, M. and Perri, E.: Calcareous bioconstructions formation during the last interglacial
929 (MIS 5) in the central Mediterranean: A consortium of algal, metazoan, and microbial framebuilders (Capo Colonna–
930 Crotone Basin South Italy). *Marine and Petroleum Geology*, 167, 106950,
931 <https://doi.org/10.1016/j.marpetgeo.2024.106950>, 2024.

932

933 Santoro, E., Mazzella, M. E., Rerranti, L., Randisi, A., Napolitano, E., Rittner, S. and Radtke, U.: Raised coastal terraces
934 along the Ionian Sea coast of Northern Calabria, Italy, suggest space and time variability of tectonic uplift rates.”
935 Quaternary International, 206, 78–101, <http://dx.doi.org/10.1016/j.quaint.2008.10.003>, 2009.

936

937 Savini, A., Borrelli, M., Vertino, A., Mazzella, F., and Corselli, C.: Terraced Landforms Onshore and Offshore the Cilento
938 Promontory (Southern Tyrrhenian Margin): New Insights into the Geomorphological Evolution, *Water*, 13 (4), 566,
939 <https://doi.org/10.3390/w13040566>, 2021.

940

941 Savini, A., Vertino, A., Marchese, F., Beuck, L. and Freiwald, A.: Mapping cold–water coral habitats at different scales
942 within the Northern Ionian Sea (central Mediterranean): An assessment of coral coverage and associated vulnerability.
943 PLoS ONE, 9, e87108. <https://doi.org/10.1371/journal.pone.0087108>, 2014.

944

945 Schlager, W.: Accommodation and supply–A dual control on stratigraphic sequences. *Sedimentary Geology*, 86, 111–
946 136, 1993.

947

948 Schlager, W.: Depositional bias and environmental change–important factors in sequence stratigraphy. *Sedimentary*
949 *Geology*, 70, 109–130, 1991.

950

951 Sciuto, F., Altieri, C., Basso, D., D’Alpa, F., Donato, G., Bracchi, V. A., Cipriani, M., Guido, A., Rosso, A., Sanfilippo,
952 R., Serio, D. and Viola, A.: Preliminary data on ostracods and foraminifers living on coralligenous bioconstructions
953 Offshore Marzamemi (Ionian Sea, Se Sicily). *Revue de Micropaléontologie*, 18, 100711,
954 <https://doi.org/10.1016/j.revmic.2023.100711>, 2023.

955

956 Severino, U., Lagudi, A., Barbieri, L., Scarfone, L., and Bruno, F.: A SLAM–Based Solution to Support ROV Pilots in
957 Underwater Photogrammetric Survey. In *International Conference of the Italian Association of Design Methods and Tools*
958 *for Industrial Engineering* (pp. 443–450). Cham: Springer Nature Switzerland,
959 https://link.springer.com/chapter/10.1007/978-3-031-58094-9_49, 2023.

960

961 SNPA, Methodological Sheets used in the monitoring program of the second cycle of the Marine Strategy Directive
962 (Ministerial Decree 2 February 2021) SNPA technical publications, [https://www.snpambiente.it/snpa/schede-](https://www.snpambiente.it/snpa/schede-metodologiche-utilizzate-nei-programmi-di-monitoraggio-del-secondo-ciclo-della-direttiva-strategia-marina-d-m-2-febbraio-2021/)
963 [metodologiche-utilizzate-nei-programmi-di-monitoraggio-del-secondo-ciclo-della-direttiva-strategia-marina-d-m-2-](https://www.snpambiente.it/snpa/schede-metodologiche-utilizzate-nei-programmi-di-monitoraggio-del-secondo-ciclo-della-direttiva-strategia-marina-d-m-2-febbraio-2021/)
964 [febbraio-2021/](https://www.snpambiente.it/snpa/schede-metodologiche-utilizzate-nei-programmi-di-monitoraggio-del-secondo-ciclo-della-direttiva-strategia-marina-d-m-2-febbraio-2021/), 2024.

965

966 Stephens, D., Smith, A., Redfern, T., Talbot, A., Lessnoff, A. and Dempsey, K.: Using three dimensional convolutional
967 neural networks for denoising echosounder point cloud data. *Applied Computing and Geosciences*, 5-100016,
968 <https://doi.org/10.1016/j.acags.2019.100016>, 2020.

969

970 Varzi, G. A., Fallati, L., Savini, A., Bracchi, V. A., Bazzicalupo, P., Rosso, A., Sanfilippo, R., Bertolino, M., Muzzupappa,
971 M., and Basso, D.: Geomorphology of coralligenous reefs offshore southeastern Sicily (Ionian Sea).” *Journal of Maps*,
972 19 (1), [https://doi=10.1080/17445647.2022.2161963](https://doi.org/10.1080/17445647.2022.2161963), 2023.

973

974 Vosselman, G.: Slope based filtering of laser altimetry data. IAPRS, Vol. XXXIII, Amsterdam, 2020.

975

976 Westaway, R. and Bridgland, D: Late Cenozoic uplift of Southern Italy deduced from fluvial and marine sediments:

977 coupling between surface processes and lower-crustal flow. *Quaternary International*, 175, 86–124,

978 <http://dx.doi.org/10.1016/j.quaint.2006.11.015>, 2007.

979

980 Westaway, R.: Quaternary uplift of Southern Italy. *Journal of Geophysical Research*, 98 (B12), 21741–21772,

981 <http://dx.doi.org/10.1029/93JB01566>, 1993.

982

983 Zecchin, M. and Caffau, M.: Key features of mixed carbonate–siliciclastic shallow–marine systems: the case of Capo

984 Colonna terrace (southern Italy). *Italian Journal of Geosciences*, 130 (3), 370 – 379.

985 <http://dx.doi.org/10.3301/IJG.2011.12>, 2011.

986

987 Zecchin, M., Caffau, M., Civile, D. and Roda, C.: Facies and cycle architecture of a Pleistocene marine terrace (Crotone,

988 southern Italy): a sedimentary response to late Quaternary, high–frequency glacio–eustatic changes. *Sedimentary*

989 *Geology*, 216, 138–157, <http://dx.doi.org/10.1016/j.sedgeo.2009.03.004>, 2009.

990

991 Zecchin, M., Caffau, M., Civile, D., Critelli, S., Di Stefano, A., Maniscalco, R., Muto, F., Sturiale, G., and Roda, C.: The

992 Plio–Pleistocene evolution of the Crotone Basin (Southern Italy): interplay between sedimentation, tectonics and eustasy

993 in the frame of Calabrian arc migration.” *Earth Science Reviews*, 115, 273–303.

994 <http://dx.doi.org/10.1016/j.earscirev.2012.10.005>, 2012.

995

996 Zecchin, M., Nalin, R. and Roda, C.: Raised Pleistocene marine terraces of the Crotone peninsula (Calabria, southern

997 Italy): facies analysis and organization of their deposits. *Sedimentary Geology*, 172, 165–185. doi:

998 10.1016/j.sedgeo.2004.08.003, 2004.

999

1000 Zevenbergen, L.W. and Thorne C. R.: Quantitative analysis of land surface topography. *Earth Surface Processes and*

1001 *Landforms*, 12 (1), 47–56. <https://doi.org/10.1002/esp.3290120107>, 1987.